MECHANISTIC MODEL OF VEGETATION STRUCTURE AND ANIMAL COMMUNITY INTERACTIONS-INTEGRATING GEDI & TLS DATA IN THE MADINGLEY MODEL

Camille Gaillard[1,6], Michael Harfoot[2], Andrew Abraham[3], Luca Santini[4], Patrick Jantz[1], Toby Jackson[5], Alexander Shenkin[1], Patrick Burns[1], Scott Goetz[1] and Christopher Doughty[1]

[1] School of Informatics, Computing and Cyber-Systems, Northern Arizona University, Flagstaff, USA
[2] Vizzuality, Cambridge, United Kingdom
[3] Department of Biology - Ecoinformatics and Biodiversity, Aarhus University, Aarhus, Denmark
[4] Department of Biology and Biotechnologies, Sapienza University of Rome, Rome, Italy
[5] Conservation Initiative and the Plant Sciences department, University of Cambridge, Cambridge, United Kingdom
[6]Contact author: Camille.gaillard@nau.edu

ABSTRACT

Background

Vegetation structure is increasingly recognized as a key variable to explain ecosystems states and dynamics. New Remote Sensing tools are available to complement labor intensive field investigations and consider the global biogeography of this parameter.

Objectives

We propose to model the processes explaining the interaction between vegetation structure and animal community assembly globally, while requiring minimal computing power, based on the most fundamentals assumptions.

Methods

We integrate spaceborne (GEDI: Global Ecosystem Dynamics Investigation) and ground based (TLS: Terrestrial Laser Scanning) Lidar data in the Madingley general ecosystem model. We compare the outcome of this integration to previous version and to the TetraDensity estimate of animal biomass and Elton traits database for arboreality.

Results

Animal biomass density simulated by Madingley is closer to global estimates when integrating vegetation structure. The strength of this effect increases with higher cohort body mass and varies with local environmental conditions and stochastic processes. Simulated proportion of arboreality across cohorts is

consistently higher than observations. This is consistent with the divergence of biases between model and database.

Conclusions

Our results concur with our hypotheses about the role of vegetation structure on animal community assembly, as it reduces total animal biomass abundance. However, assessing the accuracy of its relative weight is challenging. While we have global products about arboreality and animal biomass density, they represent modern day ecosystem state, including anthropogenic activity, while Madingley simulates potential ecosystem optimum. Therefore, we call for further research in this field and for challenging modelling attempts to compare with.

Keywords: Vegetation Structure, GEDI, TLS, LIDAR, Madingley, Mechanistic model, Arboreality

INTRODUCTION

Pressures on biodiversity are increasing at an alarming rate due to the combined effects of climate change and land use intensification (Newbold et al., 2016). These factors pose a significant threat not only to the future of life on Earth (Mace et al., 2014) but also to the stability and resilience of our societies (Rockström et al., 2009). To effectively address these challenges and develop appropriate strategies, models that can accurately assess and predict future scenarios are crucial, providing valuable insights to inform decision-making processes. Earth System Models (ESMs), Land-Surface Models (LSMs) and Dynamic Global Vegetation Models (DGVMs) have become key tools for ecological research and conservation (Collier et al., 2018; Eyring et al., 2016; Prentice et al., 2007, 2015). These models enable scientists to investigate complex ecological processes, such as carbon cycling, nutrient dynamics, and plant biogeography. While ESMs, LSMs and DGVMs have been widely adopted, it is crucial to acknowledge the pressing need for ecological models that also mechanistically simulate fauna. The ongoing sixth mass species extinction event, fueled by anthropogenic activities, highlights the urgency to understand and predict the fate of animal populations and their interactions within ecosystems (Barnosky et al., 2011; Ceballos et al., 2017; Cowie et al., 2022). In this context, the Madingley model stands out as a unique ecological model capable of simulating fauna in a mechanistic manner, allowing for the exploration of unprecedented future scenarios and response to the biodiversity crisis (Harfoot et al., 2014; Purves et al., 2013). However, it is currently limited by its inability to explicitly represent vegetation structure. This means that it represents vegetation as a flat ground layer, which is a relatively correct approximation across grasslands, but challenging when simulating forests. Thanks to advancements in technology and new on-the-ground observations and remote sensing products, we have new opportunities to solve this limitation. By incorporating these emerging data sources into model development, we can improve simulations accuracy and enhance our ability to investigate the complex interactions between animal communities and vegetation structure, factoring biodiversity, climate change, and land use.

The role of vegetation structure in ecological processes is increasingly studied and acknowledged. It has been identified as the main driver of overall ecosystem productivity (Migliavacca et al., 2021), and linked to numerous ecological dynamics. It has been linked to biophysical processes, such as fire regime (Just et al., 2016; Veenendaal et al., 2018) or hydrology (Wu et al., 2022; Zhu et al., 2012), as well as ecosystem functional traits and energetics (Campos-Silva & Piratelli, 2020; Migliavacca et al., 2021;

Russo et al., 2023; Stark et al., 2015; West et al., 2009), and particularly shaping biodiversity through biotic dynamics (Srivastava, 2006; Tilman et al., 2014), from plant interactions (Dohn et al., 2017; Franklin et al., 2020; Martínez Cano et al., 2020) to habitat and niche partitioning for animal species (Gámez & Harris, 2022; MacArthur & MacArthur, 1961; Salas-López et al., 2022; Ye et al., 2021). Yet, there is no comprehensive consensus about the overall importance of vegetation structure in ecosystem states and dynamics, as its role is complex (Coverdale & Davies, 2023; Russo et al., 2023). Landscape complexity, including vegetation structure, would benefit from additional investigations to explain animal biogeography (e.g.: range dynamics (Heit et al., 2021)). Obtaining precise observations about this relation is challenging at global scale (Killion et al., 2023a). We propose to advance this field by integrating 3-dimensional vegetation structure in a mechanistic global ecological model, to simulate its influence on animals' biogeography. Such research has been limited until recently by data scarcity. Obtaining observations about vegetation structure at large scale, and tree architecture in particular, has been historically challenging. However, new methodologies and tools are bridging this gap (Atkins et al., 2022; Ishii et al., 2004; McElhinny et al., 2005). The precise branching of individual trees can now be captured thanks to ground-based TLS (Terrestrial Laser Scanning) (Lau et al., 2019a; Verbeeck et al., 2019). Such new data informs our understanding of vegetation structure in regard to tree mechanical architecture (Jackson et al., 2019; Verbeeck et al., 2019). A global measurement of vegetation structure, at the 25m resolution is also available thanks to the NASA Global Ecosystem Dynamics Investigation (GEDI) mission. Insights on the relation between tree height, branch radius, branch strength, and weight carrying capacity allow us to integrate key vegetation structure parameters in mechanistic models and simulate their influence on arboreal communities.

Understanding the global biogeography of the interplay between diverse species, and particularly between autotrophs (typically plants) and heterotrophs (herbivores, carnivores, mixed feeders) is at the heart of ecology. It is also critical to understand the consequence of anthropogenic activity and mitigate its negative impacts.

In this study, to enhance our ability to investigate the interaction between vegetation structure and animal community assembly, we combine new on-the-ground observation and remote sensing products, with the capabilities of Madingley. Our approach enhances understandings of vegetation structure influence on animal community assembly, biogeography and ecosystem functioning. We test how integrating vegetation structure into the Madingley model can shape its ability to simulate animal communities' biogeography. We question how landscape complexity, driven by plant architecture, can influence the availability of resources and shelter, thereby shaping animal populations distribution.

The more forested a region, the more relevant this work is. This expands the range of future scenarios we can investigate and provide crucial insights into the potential impacts of climate change and land use intensification on biodiversity, enabling policymakers and conservation practitioners to make informed decisions for the preservation and sustainable management of our planet's ecosystems.

METHODS

MADINGLEY

The Madingley model is a process-based model simulating cohorts (i.e. group of individuals) representing an ensemble of fauna "species" sharing the same characteristics (Harfoot et al., 2014). Each

cohort has a unique set of traits (e.g.: diet) and state parameters (e.g.: age) assigned to it, such as predation rate, body mass, and metabolic rate. These cohorts interact with each other either directly via predator-prey interaction, or indirectly, by competing for resources. They are also driven by environmental parameters, the first among them being resource availability, which is calculated in Madingley according to climatic data (M. J. Smith et al., 2013) processed internally according to the Miami model (Lieth, 1973). Other environmental parameters impact these cohorts either directly, e.g.: temperature impacts metabolic rate, or indirectly, e.g.: Mean Annual Precipitation (MAP) drives primary productivity. The model simulates community assembly processes according to these mechanisms and parameters and produce an assemblage adapted to prevailing environmental conditions and biotic interactions.

The Madingley model was first developed assuming an unstructured vegetation, which implies being spatially explicit only on a two-dimensional space. It was made to represent a common pool of biomass available to all cohorts equally. This bias is particularly concerning in forests where it leads to a simulated overabundance of large animals and a relative imbalance in community assembly. We improve community assemblages simulated by Madingley in forests by integrating vegetation structure according to Figure 1.

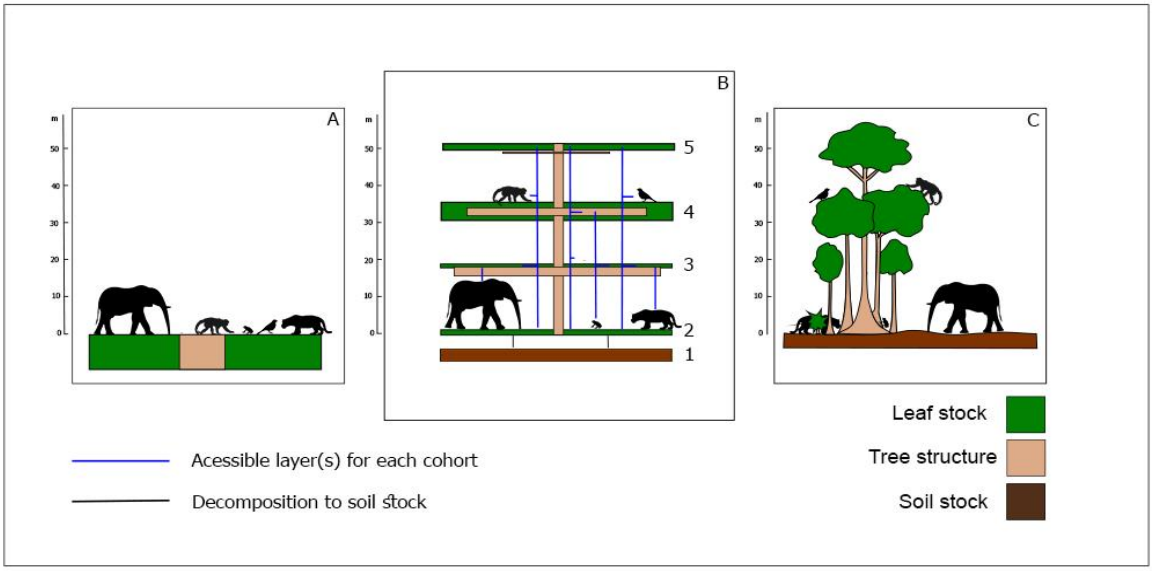

Figure 1: A) Previous master version of Madingley. The entirety of the simulated NPP is available to all cohorts equally. B) Updated 3D version of Madingley. Simulated biomass is partitioned per 5m height bin according to observations (GEDI and TLS) and made accessible to cohorts depending on vegetation structure (i.e. mechanical carrying capacity) and on cohorts' body mass.

3D VEGETATION STRUCTURE DATA

We integrate 3D vegetation structure into Madingley, at a global scale, based on TLS and GEDI data sets presented below. These data have varying spatial resolution, which we scale to our simulation's resolution. They also have varying time scopes, assumed to have minimal impact on our methodology. We consider variables from TLS assumed to be invariant with time, representing fundamentals of forest

structure. GEDI data are aggregated over 3 years of observation (the instrument started collected data from March 2019 until January 2023), which could have an impact locally due to land use change, deforestation and afforestation, which we assume can be disregarded at the 0.5° resolution. GEDI data represent vegetation 3D structure at present and will likely require updates in the future with land cover change.

TLS DATA

We gathered TLS data from 12 sites across the tropics each capturing several trees of varying size, but all with Diameter at Breast Height (DBH) larger than 15cm (Table1). For each of these trees, a cylinder model was fitted, representing the individual stem and branches position in space. These data were processed according to established methodology (Jackson et al., 2019; Lau et al., 2019b; Verbeeck et al., 2019), with the TLS cloud point being converted to cylinder models and branches being considered as a sum of each series of cylinders starting at the stem.

Table 1: Sites where TLS data was obtained (Jackson et al., 2019; Lau et al., 2019b; Verbeeck et al., 2019).

Site name	Country	Latitude	Longitude	Year	Area (ha)
Lope	Gabon	-0.1770	11.5730	2016	1
Sepilok	Malaysia	5.8698	117.9363	2017	1

The cylinder model computed from the measured TLS data gives us the maximum branch radius relative to branch height. This relation varies across sites and sampled individuals, but an aggregated regression gives significant statistical robustness (Figure 2). The data has been aggregated into 5m bins to match with GEDI 5m bins. We obtained branch length from tapering function deriving branch length from branch radius (Dahle & Grabosky, 2010).

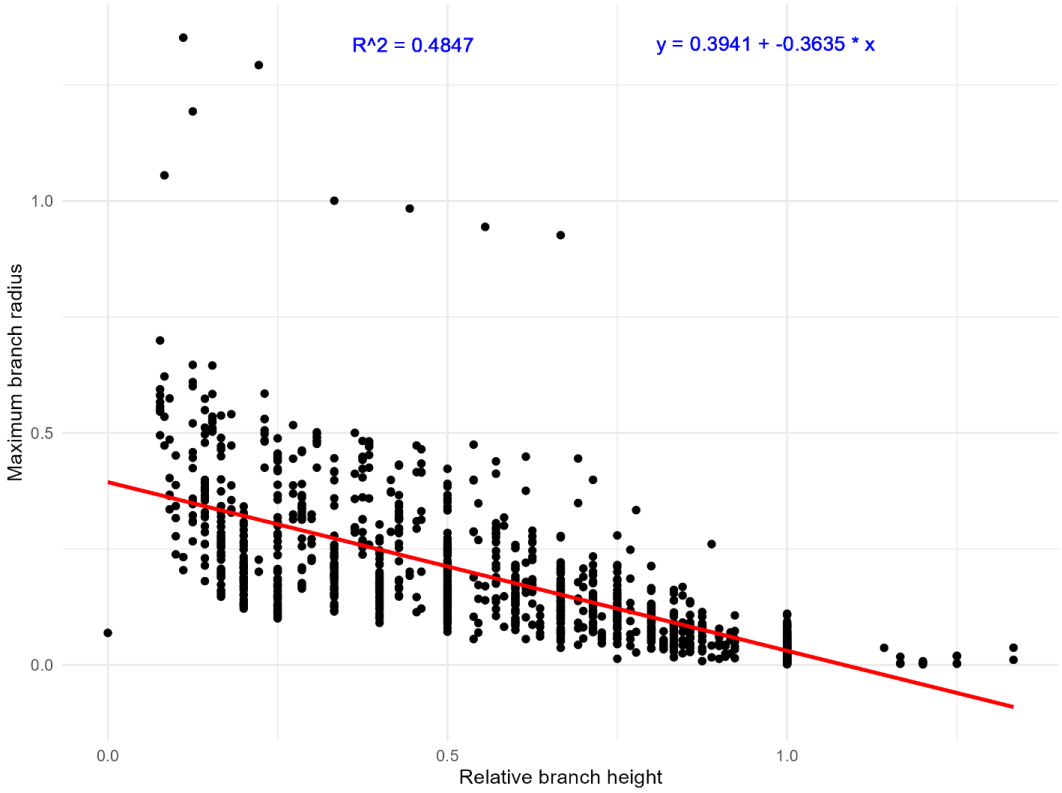

Figure 2: Relation between maximum branch radius and branch height relative to tree height.

GEDI DATA

The Global Ecosystem Dynamics Investigation (GEDI) is a NASA mission that makes use of a light detection and ranging (lidar) instrument mounted on the International Space Station (ISS). The mission produces measurements of vegetation structure and topography within the orbital domain of the ISS, between approximately 52° North and South latitude (Dubayah et al., 2020). Individual lidar returns have a 25 m diameter geolocated footprint, and for every orbit returns are spaced by 60 m along-track and 600 m across-track. We downloaded the entire GEDI L2A (Dubayah, Hofton, et al., 2021) and L2B (Dubayah, Tang, et al., 2021) dataset from the LPDAAC and used a quality-filtering recipe similar to the recipe used for the GEDI L4B product (Dubayah et al., 2022) which yielded 7.7 billion quality shots from April 2019 to March 2023. From the L2A dataset, we extracted the relative height of 98th percentile of returned energy which is a proxy for vegetation height. We use the L2B estimates of Plant Area Volume Density (PAVD) which are derived from the L1B waveform and have a vertical resolution of 5 m. PAVD represents the amount of vegetation material in each height bin; notably, it includes woody material like branches and trunks.

We processed RH98 (overall vegetation height) and the vertical PAVD profile from 0 to 60 m to fit our specific needs by aggregating them to a spatial resolution of 0.5 decimal degrees. To do this, we first computed a 1 km resolution (~ 0.009°) raster corresponding to the mean value of all quality GEDI shot metric values. For each metric, we then averaged all of the 1 km pixel values within each 0.5° grid cell. Finally, we transformed the PAVD profile to relative fraction of PAVD per height bin. Collating GEDI data at the 0.5° spatial resolution is necessary for computationally tractable simulations at the regional to global

extent and it improves the statistical validity of the measured PAVD profile, compared to disparities between the native 1 km GEDI grid cells (Figure 3). This relates to a well-known issue of sampling density. For example, Béland et al. (2014) show that LIDAR data displays varying values of Leaf Area Density depending on spatial resolution and sampling volume; and this depends on leaf size and branch architecture, thus varying regionally and per species.

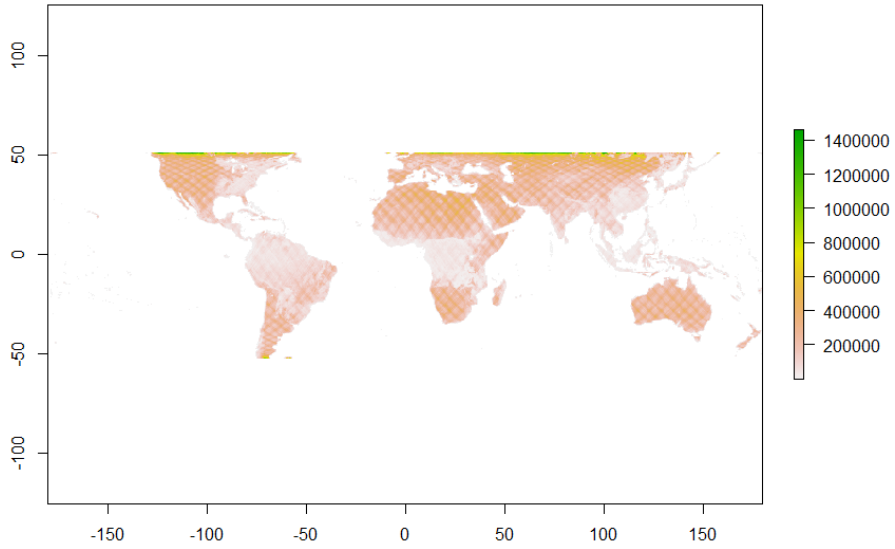

Figure 3: Number of GEDI returns per 0.5° from April 17th, 2019, to March 17th, 2023.

3D VEGETATION STRUCTURE INTEGRATION IN MADINGLEY

To integrate vegetation structure in Madingley, we need to align the complexity of vegetation structure with the architecture of Madingley. This implies to make reasonable assumptions to simplify the representation of vegetation structure and its interaction with animal population in computationally tractable framework.

SINGLE LARGEST TREE

The first assumption we make to integrate vegetation structure into Madingley is to assume a single largest tree approach. In each simulated grid-cell, forest structure is represented by an archetypal tree corresponding to the tallest tree measured. This assumption follows general quantitative theory of forest structure and dynamics (West et al., 2009), which states that properties of trees (geometric and dynamic) scale linearly, allowing us to represent a forest stand as a scaled version of the tallest tree. This also follows measurements showing that largest trees disproportionately contribute to leaf area and forest functioning (Enquist & Niklas, 2001; Taubert et al., 2021). Finally, this is a necessary assumption considering that GEDI provides a canopy height map and not a measure of each individual tree height. This archetypal

largest tree is integrated into Madingley based on GEDI and TLS data and according to structural equations of plant physics following Figure 5. Similarly to the largest tree assumption, we consider only the largest branches. For three reasons. First, as we consider the largest tree, we have to consider the largest branch for consistency. Second, this is a proxy for arboreality adaptation. As animals adapted to navigating complex 3D environments, they developed traits allowing them to minimize its challenges and to take advantage of it (e.g.: spreading their weight across multiple points or branches, or reaching thinner branches from the safety of a larger one). Third, Madingley runs with a timestep resolution of 1 month, during which we can assume that cohorts experience branches of different sizes. This is reinforced by the fact that each simulated cohort represents a number of individuals. This point implies that simulated cohorts, at the 1-month time scale, can sample the whole landscape and maximize their access to its resources.

This single largest tree approach implies a higher resource availability for each simulated cohort *vs.* what would be available considering the full spectrum of tree and branch sizes. This approach is also motivated by the lack of completeness in information availability about forest structure. GEDI PAVD is useful to allocated vegetation through the height column and measure the highest point, but it does not directly inform about the mixture of trees of different sizes. Similarly, the TLS data available is usually constrained to trees with a DBH>10-15cm typically.

The height of this simulated archetypal largest tree in a grid-cell is informed by the GEDI RH98 height map (Dubayah, Hofton, et al., 2021). We aggregate multiple signal points at the scale at which we run our simulations by averaging the maximum GEDI RH 98 across the grid-cell, representing top of the canopy. As every 0.5 ° grid-cell encompasses a different number of GEDI point, each has a different statistical validity (Figure 3). Branch sizes at each 5m height bin are informed by TLS data presented above.

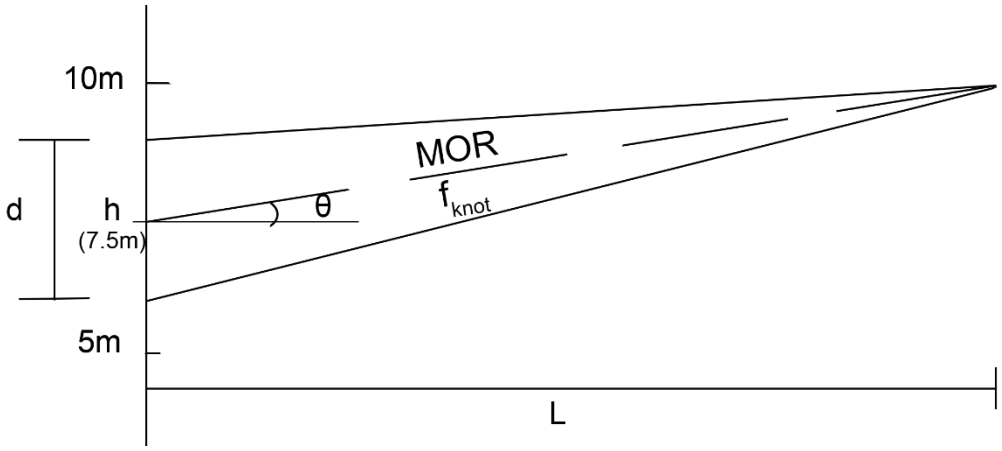

Figure 4: Schematic representation of the simulated archetypal tree and associated variables.

STRUCTURAL EQUATIONS

We calculate the canopy space each cohort can access according to their body mass and structural equations determining branch load bearing capacity. Following plant physics and biomechanics (Niklas & Spatz, 2012), we calculate the maximum weight a branch can carry depending on its dimensions, according to the following equations. A branch breaks when load equals or exceeds its breaking point. A branch load is calculated as follows:

$$M_{load} = m_{animal} \cdot l \cdot g \cdot \cos(\theta) \quad (1)$$

Where M_{load} is the moment at the base of the branch, l is the distance along a branch where an animal of mass m_{animal} sits, g is the acceleration due to gravity, 9.81 , and θ the angle of the branch from the horizontal. Here, we assume branch angle to be constant for all branches, globally, assuming straight branches without further bends. The breaking point of a branch, or branch strength is calculated as follows:

$$M_{break} = \frac{\pi}{32} f_{knot} \cdot MOR \cdot d^3 \quad (2)$$

Where d is the branch diameter, MOR is the modulus of rupture and f_{knot} is a factor accounting for measurements limitations. MOR is typically measured on undamaged wood, whereas real branches contain defects. Here, we use a value of 0.8 for f_{knot}, as it is commonly used (Moore et al., 2009). Thus, a branch breaks if M_{load}=M_{break}, giving us the maximum weight of any animal individual trying to access any given point along any given branch. It can be calculated as follows:

$$m_{animal} = \frac{\pi f_{knot}}{32g} \cdot \frac{d^3 MOR}{l \cos(\theta)} \quad (3)$$

In these relations, we do not account for branch self-weight. We also assume branches to be cylindrical to simplify calculations, as it is a common assumption (Hackenberg et al., 2015; Raumonen et al., 2013). Finally, we do not consider sub-branching, as it would add further unnecessary and unwieldy uncertainties. Thus, implicitly assuming that sub-branches are split evenly sized. We sum up the branch length accessible to a cohort at each height bin to obtain the total branch space it can access, in proportion of the total branch space available.

PRODUCTIVITY PARTITIONING

Madingley simulates plant productivity (or autotroph biomass) according to environmental variables. We partition this productivity across the height column divided in 5m bins proportionally according to the GEDI PAVD profile. We further spread this autotroph biomass along branch length according to a linear relation relative to branch length.

INTEGRATION FRAMEWORK

A comprehensive overview of integration of the above presented points is given in Figure 5, and as follows. GEDI data is read in Madingley to inform two points. ***1.*** One, for each simulated grid-cell, in each 5m height bin, the PAVD fraction is read in Madingley (R. Dubayah, Tang, et al., 2021). ***2.*** This PAVD fraction is converted in the fraction of simulated net primary productivity (NPP) allocated to each height bin. NPP is simulated in Madingley according to the Miami model (Lieth, 1973). ***3.*** Two, GEDI tree height is read similarly, but as a unique value, for each grid cell. ***4.*** TLS data inform us about the ***5.*** relation between maximum branch diameter and branch height. Tree height is used to determine the number of 5m vertical bins and, in conjunction with TLS data, to calculate branch sizes: ***6.*** Maximum diameter at each height bin and ***7.*** Associated length in each bin according to empirically derived relation from available TLS data (see Table 1 and Figure 2) and considering the archetypal largest tree simplification. ***5.*** & ***6.*** Given tree height, we can calculate branch radius (considering the largest branch) at each height bin. ***7.*** Branch length is derived from the maximum branch radius (at the base of the branch), according to a tapering function (Figure 4). ***8.*** The branch strength equations ((1) (2) & (3)), are used to calculate for each cohort,

9. based on its individual body mass, ***10.*** the branch space it can access. ***11.*** NPP is distributed along branch length and ***12.*** accessible to each cohort according to the branch space it can access.

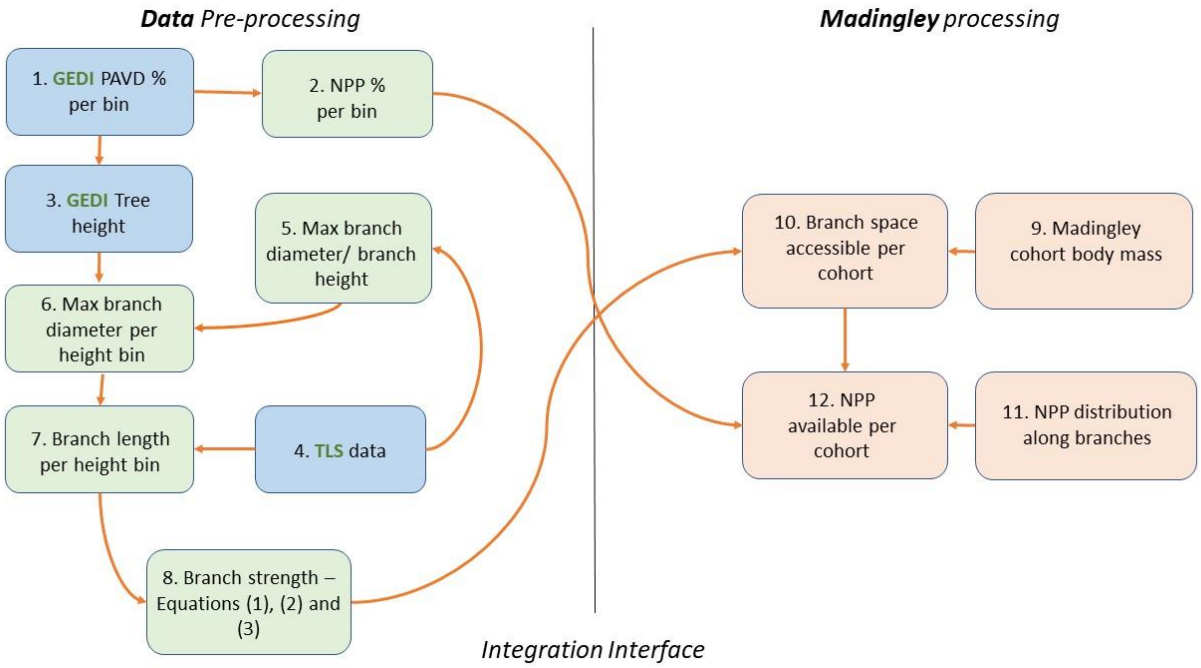

Figure 5: Schematic representation of our methodology to integrate data. The boxes right of the Madingley interface line are calculated in the model at each time step for each cohort, while boxes left of this line are pre-processed.

FEEDING BEHAVIOUR & PREDATION

We assume that each cohort feeds evenly across all the space it can access, depending on the relation between its body size and branches architecture. Concomitantly, we assume it spends its time where it feeds. This assumption discounts other activities, which could drive where animals spend their time, such as nesting and travelling between feeding sites. This simplification is however necessary as there is currently no complete picture of animal behavior, and time spending specifically, which could mechanistically be linked to traits and variables.

Similarly, we calculate the preys a predator cohort can access according to its individual body mass by determining the branch space it can access and the percentage of overlap it has with the branch space accessible for each of its preys. Again, we assume that each cohort occupies indiscriminately all the branch space it can access. Biomass taken by predator cohorts from prey cohorts is then removed from the overall prey cohort biomass, as in previous Madingley version, albeit adjusted by the vegetation structure factor (Figure 6).

In details, we sum the branch space accessible ***1.*** for a prey and ***2.*** for its predator and ***3.*** the percentage of overlap is calculated and ***4.*** used to reduce proportionally the prey biomass available to a

predator. Considering ***5.*** predator feeding needs and ***4.*** adjusted prey availability, ***6.*** target prey cohort biomass is removed.

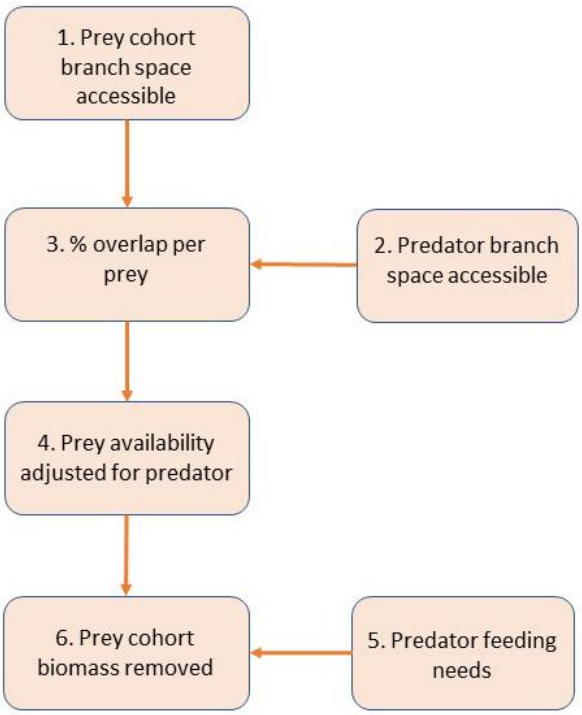

Figure 6: Schematic representation of our methodology to simulate arboreal predation while considering vegetation structure.

SIMULATIONS & ASSESSMENT

To evaluate the relevance of our modelling approach we compare simulation results obtained with our new updated version of Madingley (hereafter 3D version), integrating vegetation structure to simulation results obtained with the original version of Madingley (Harfoot et al., 2014) (hereafter 2D version). We also compare them to relevant external datasets and reanalyses. First, against animal density data from the TetraDENSITY database (Santini et al., 2018). Second, against arboreality biogeography from the Elton trait database (Wilman et al., 2014) as analyzed in Jantz et al., (2024). We performed simulations, with both 3D and 2D versions (for Amazon, Congo and Borneo sites, Table 2) to test simulated animal biomass against TetraDensity. We performed simulations with the 3D version for forested and for open landscapes (African Forest and African Savanna, Table2) to test arboreality against Elton traits database. Simulations were conducted at the 0.5° resolution. These site-specific simulations are to test the effect of vegetation structure specifically. We ran each simulation for 100 years to allow for simulations to reach a dynamic equilibrium. We made 3 replicates of each simulation to account for stochasticity.

Table 2: Sites for which simulations were conducted.

Site ID	Longitude	Latitude
Amazon	-51	-2
Congo	13	1
Borneo	112	0
Africa Forest	11 to 14	0 to 3
Africa Savanna	32 to 35	-3 to -6

We have three key targets to assess the performance of our approach. First, we consider the distribution of cohort body mass classes and total simulated cohorts' biomass. Including vegetation 3D structure should increasingly reduce the abundance of cohorts with increasing individual body mass. Second, we consider how simulated animal population densities compare to observations and processed data by benchmarking our results against the TetraDENSITY database (Santini et al., 2018). Third, we assess how simulated distribution of arboreal animals matches with biogeography of the arboreality trait from the ELTON trait database, as highlighted by Jantz et al. (n.d.).

DATASETS

TetraDENSITY

As an independent validation of the global biomass pattern that emerges from the Madingley, we estimated biomass for endotherms globally using population density predictions combined with IUCN Red List range polygons (IUCN, 2022). We obtained population density predictions for 4925 species of mammals and 9108 species of birds from Santini et al. (2022) and Santini et al. (2023), respectively. We generated a parse matrix of species presence based on IUCN range polygons at 50km resolution in Mollweide equal area projection. For migratory birds, we used the breeding and resident range only. We then multiplied the area per cell with the average density of each species present to obtain an estimate of species abundance per cell. Subsequently, to obtain biomass we multiplied the abundance by the respective species body mass derived from EltonTraits (Wilman et al., 2014). Since the Madingley models endotherms with no distinction between birds and mammals, we summed up the biomass of all bird and mammal species per cell to obtain a first approximation of total endotherm biomass per cell. Clearly, this is a coarse approximation that does not consider available habitat per species within cells, but it is acceptable for comparisons of geographic patterns with the Madingley which models organisms' biomass at a low resolution with no consideration of habitat within cells. Further, we are not interested in the absolute values but rather in the relative differences. For example, we expect to see greater gaps between Madingley and modern world estimates, in regions where large mammals have suffered important range contractions (e.g. Elephants in Africa). We did not model biomass of amphibians and reptiles as population density estimates available (Santini et al., 2018) are more scarce and biased toward few regions.

Arboreality

The Elton traits database contains information about arboreality as a trait (Wilman et al., 2014). Jantz et al. (n.d.) shows the global distribution of this trait per animal group and relatively to other traits. We compare this trait distribution to the number of cohorts and the proportion of cohorts simulated by

Madingley as arboreal. We categorize a cohort as arboreal if its residency time (based on where it feeds) is entirely spent above the 0-5m bin, as scansorial if it shares its time between ground (0-5m bin) and arboreal locations (disregarding relative time spent in each). Arboreality is defined by time spent foraging in trees in the Elton trait database, i.e. a species is arboreal if it forages mainly in trees. We also compare how arboreality varies with individual body size, as simulated by Madingley and as observed in the Elton trait database.

RESULTS

Simulation results obtained with the 3D version of madingley, for three sites across tropical forests, show lower total animal cohort biomass, across individual body mass range, compared to the 2D version of Madingley (Figure 7). This brings Madingley simulations outputs closer to global modern day estimates according to TetraDensity data (Santini et al., 2022, 2023). While this effect is overall true across tested sites, its strength varies and can even in some cases bring simulated biomass below modern-day estimates. We categorized cohorts in individual body size classes (i.e.: each class can contain multiple cohorts). Doing so shows that the reduction of cohorts' biomass induced by incorporating vegetation structure in Madingley's simulations is greater for larger bodied cohorts (Figure 7). This is in line with literature, showing preferential extirpation of larger animals by anthropogenic activity (e.g.: Hill et al., 2020). We expect Madingley's outputs not to be identical to TetraDENSITY estimates, as they represent present day animal biomass density, while Madingley simulates potential optimal animal biomass density based on climatic variables. However, we do not have sufficient information to accurately assess the relative weight of this effect across sites and individual body sizes.

Simulations results produced with the 3D version of Madingley display a higher variability in terms of total cohorts' biomass, across body size classes and sites, compared to results obtained with the 2D version. This reflects the greater stochasticity potential due to cohorts distribution through the vertical column.

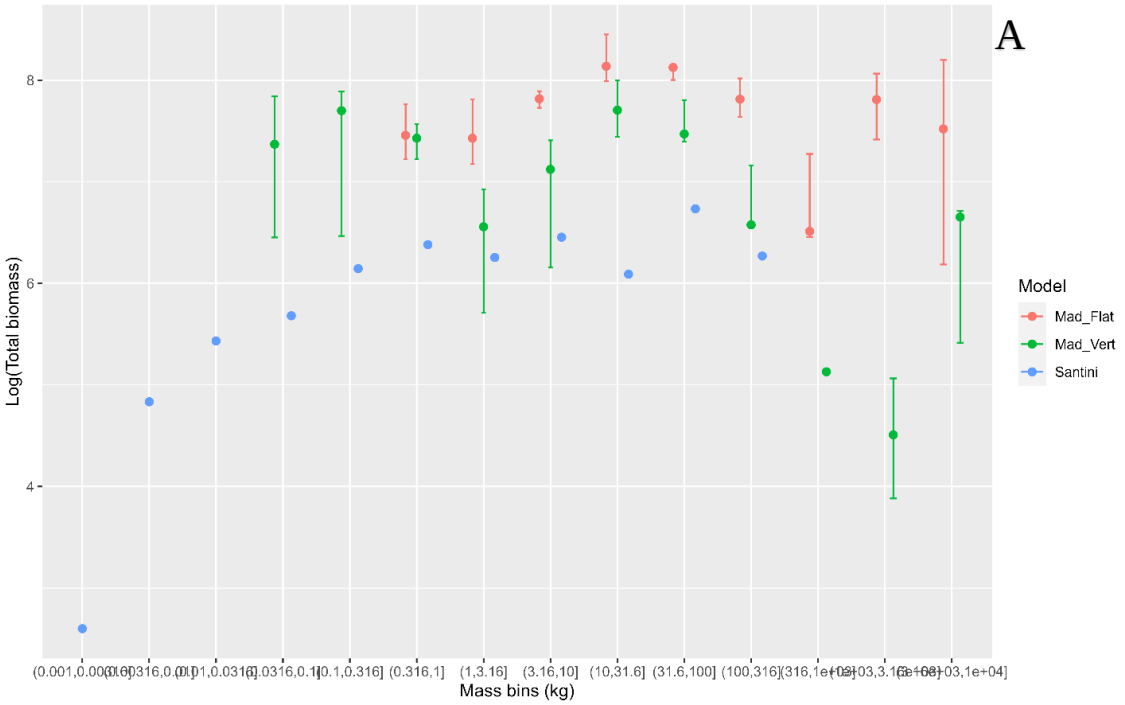
A
Log(Total biomass)
8
6
4
(0.001,0.00
(0.0
316,0.00
(0.01,0.0316]
(0.0316,0.1]
(0.1,0.316]
(0.316,1]
(1,3.16]
(3.16,10]
(10,31.6]
(31.6,100]
(100,316]
(316,1e+03]
3,3.16
(3e+03,1e+04]
Mass bins (kg)
Model
Mad_Flat
Mad_Vert
Santini

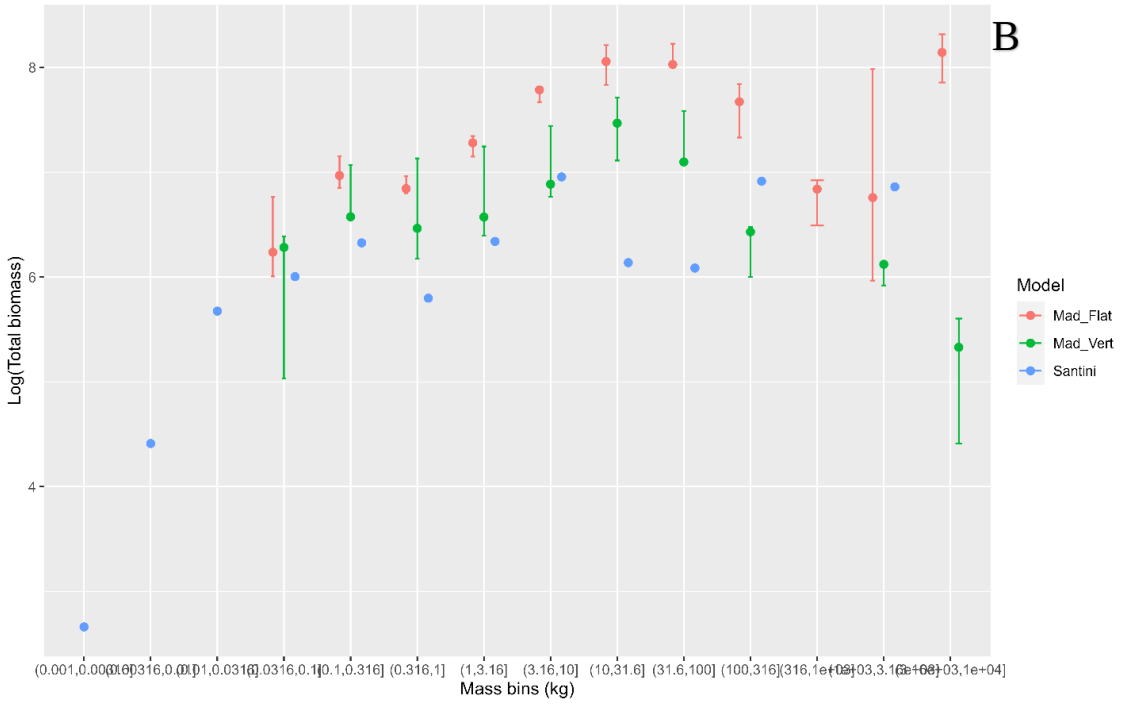
B
Log(Total biomass)
8
6
4
(0.001,0.00
(0.0
316,0.00
(0.01,0.0316]
(0.0316,0.1]
(0.1,0.316]
(0.316,1]
(1,3.16]
(3.16,10]
(10,31.6]
(31.6,100]
(100,316]
(316,1e+03]
3,3.16
(3e+03,1e+04]
Mass bins (kg)
Model
Mad_Flat
Mad_Vert
Santini

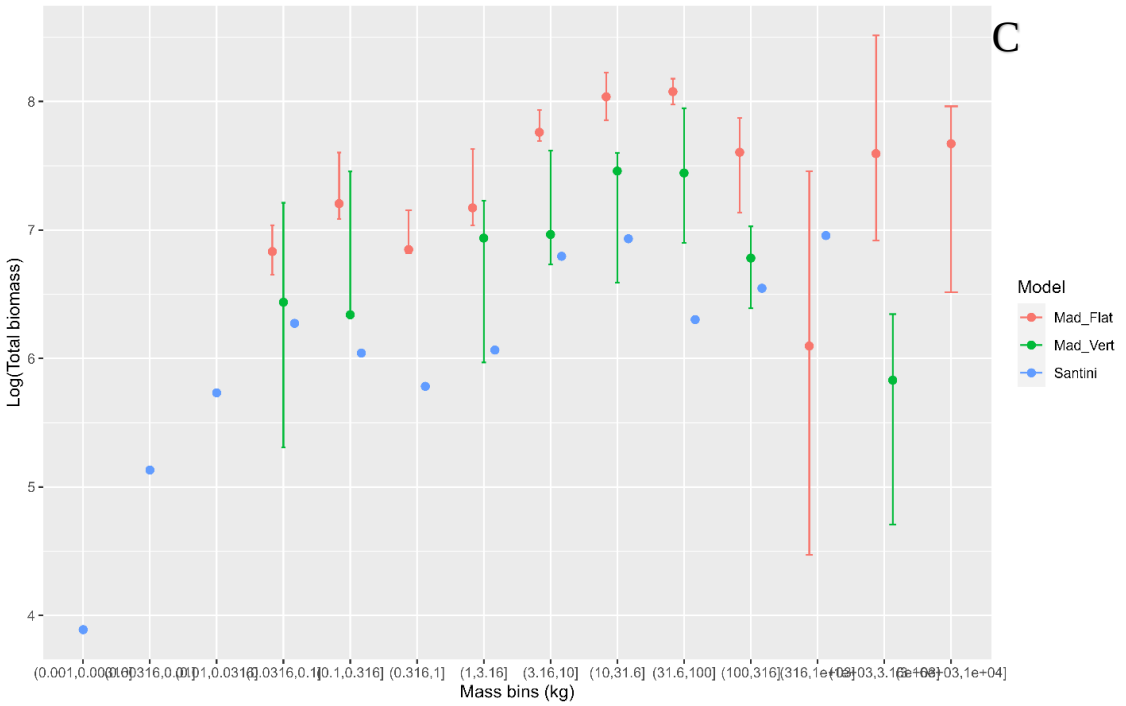

<u>Figure 7</u>: Distribution of total biomass abundance of endotherm cohorts in function of cohort individual body masses (in kg), for three forest sites across the tropics according to TetraDensity estimates (Blue) and as simulated by Madingley previous 2D version (Red) and by Madingley newer 3D version (Green). A): Amazon, B): Borneo, C): Congo

While the 3D version of Madingley simulates a percentage of arboreal cohorts in range with the percentage of arboreal species, as listed by the Elton traits database (Jantz et al., 2024), it is consistently higher (Figure 8). This is sensitive to the categorization of arboreal species we use to analyze Madingley's outputs (results not shown). The Elton traits database provides arboreality in function of time spent in the canopy, counting every activity, including travelling and sheltering. While this includes foraging, Madingley can only consider foraging at the moment to compute residence time. The direction of this bias is challenging to evaluate. Moreover, Madingley simulates cohorts, which can represent multiple species sharing a similar combination of traits, thus altering its ability to represent biodiversity metrics commensurate with field observations.

Another mismatch in calculating percentage of arboreality between the Elton traits database and madingley is that the database is skewed towards larger animals, while Madingley simulates equally cohorts of any body size. This implies an increasingly large disconnection for increasingly smaller species. Typically, insects are less restricted in their arboreality by Madingley, due to their small individual bodymass, and are less represented in the database. This concurs with Madingley simulating higher percentages of arboreality compared to database.

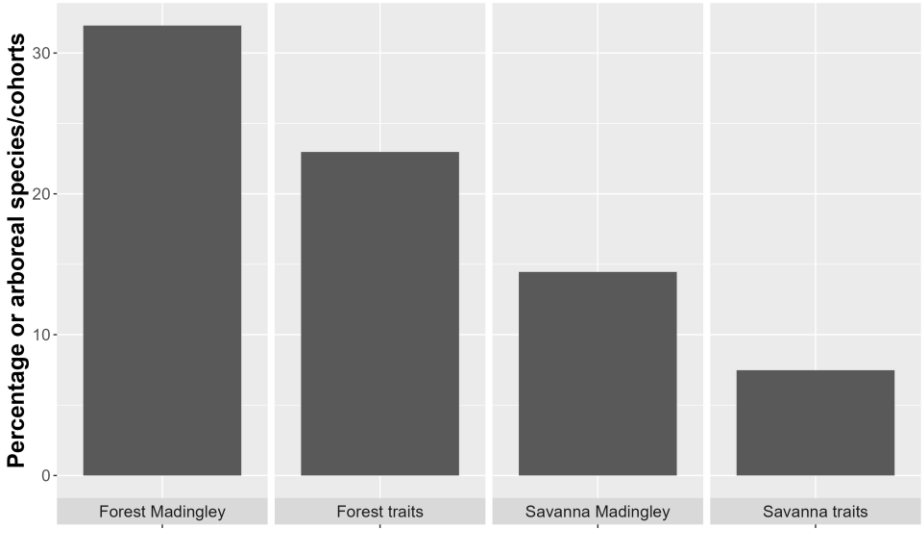

Figure 8: Percentage of arboreal cohorts, and species as simulated by Madingley 3D, and as provided by the Elton traits database (Jantz et al., 2024), respectively.

DISCUSSION

Direct results discussion:

The 3D version of Madingley produces outputs more closely aligned with observations from TetraDENSITY. This means that Madingley is now able to produce more realistic abundance density thanks to its integration of vegetation structure, specifically for smaller species. Thus, the 3D version of Madingley is more accurate than the previous 2D versions for simulations targeting forested areas and smaller species.

Madingley simulates consistently higher biomass than what the TetraDENSITY shows, across body size classes, but difference is decreased with decreasing body size. This pattern is reinforced when grouping birds with mammals from TetraDENSITY. This is likely explained by the human impact on animal populations, which has historically affected larger species disproportionately more than smaller ones (Bergman et al., 2023; Lemoine et al., 2023; Sandom et al., 2014), but this trend is still debated (Stewart et al., 2021). According to this hypothesis, as Madingley simulates potential optimal community assembly based on environmental conditions and energetics it should display an overall increasing gap with observations for increasing species body sizes. The strength of this effect could be greater than shown in this study, as it has been shown that the Miami model, as embedded in the Madingley model, leads to an underestimation of productivity, and biomass in tropical forests relatively to savanna.

Data integration & Future scenarios of vegetation structure

Some of the spatial discrepancy between observed (or derived) and simulated animal communities could be explained by Madingley simulation of potential optimum or natural ecosystems. It simulates NPP in each grid cell based on prevailing environmental conditions, ignoring land use and land use change (Harfoot et al., 2014). This allow for simulating future climatic scenarios, but, depending on site specific conditions, it can produce higher NPP to feed animal populations than what is available considering human

impact. Anthropic appropriation and modification of NPP indirectly modify animal community assembly, which is further directly impacted by human activity (e.g. hunting, trapping). To circumvent this issue, indices of human impact or anthropization, such as (Haberl et al., 2007; Krausmann et al., 2013; Newbold et al., 2020), can be included in Madingley's simulations. However, they do not directly inform processes simulated by Madingley, but only adjust them. They typically lack precision to be mechanistically considered. For example, the Human Footprint or Human Influence index (Hill et al., 2020; Leu et al., 2008; Lu et al., 2023; Watson & Venter, 2019; Woolmer et al., 2008) represents human footprint, but does not discriminate between deforestation and forest plantation. As we integrate vegetation structure based on present day measurements, we could consider constraining simulated biomass by present days observations to avoid simulating forest level biomass in grid cell where no forest is observed anymore at present. This could be more precise than the human footprint index. However, this would imply assuming a relation between GEDI PAI (Plant Area Index) or total PAVD and NPP, which we have no certainty of at present. As we currently lack a correlation between vegetation structure and vegetation productivity, we are unable to mechanistically integrate it in Madingley and adjust simulated NPP according to PAVD profiles.

Further research on this question is required to advance our understanding of the mechanistic relation between vegetation structure and productivity. Investigating the impact of seasonality and inter-annual variations on GEDI PAVD pattern could provide relevant insights into this. Going further, we could also envision discriminating GEDI PAVD between leaves and branches and thus adjusting NPP per height bin based on the ratio between branches and leaves and adjusting leaves productivity based on their locations in the canopy. Studies informing about this pattern exist but they are not global or mechanistic (Nelson et al., 2014). This last point could integrate knowledge from external sources, consider the light extinction coefficient (Vose et al., 1995), but also going further and considering precise 3D leaves distribution and sun flecks (W. K. Smith & Berry, 2013; Way & Pearcy, 2012). However, for such understanding to allow for simulating future scenarios would require to be able to simulate how PAVD profile will be impacted by climate change and land use change. The first point is still far from being resolved, while the second point is investigated by an increasing number of studies, particularly regarding logging, forest management, bioregions or biotic interactions (Atikah et al., 2021; Decuyper et al., 2018; Doughty et al., 2023; Felton et al., 2006; Keany et al., 2023; Moorthy et al., 2018).

Architecture

To integrate vegetation structure in our simulations, we had to make assumptions to simplify trees and forests architecture. These simplifications are also necessary from an ecological perspective as data are lacking to provide a comprehensive picture of every parameter of vegetation structure globally. While GEDI is a near global product, but does not provide a continuous ground cover, due to its resolution and cloud cover. We limit the impact of this precision by aggregating it at higher scale. Its vertical resolution is sufficient to distribute PAVD vertically, but it is not sufficient to explore precise branching architecture. We bridge this gap by bringing in TLS data. However, these data are only available for a limited number of trees across a handful of sites We pool these data together to increase our confidence in their representativity. The relations between branch and tree sizes displayed by the TLS data we obtained appear to be context dependent (result not shown), but the importance of this effect remains to be determined. Further studies, considering more sites, will be required to assess the accuracy of our integration of vegetation structure in Madingley in this regard.

We identify the following parameters as the most directly relevant in this perspective: branching angle, branch dimensions, modulus of rupture and tree size classes distribution. The first two items require

the precision of TLS measurements, which implies to multiply field studies. The third item has been measured in several studies(Antony et al., 2011; Baar et al., 2015; Høibø & Vestøl, 2010; Rahardjo Daryl Lee Tsen-Tieng, 2014), but its global biogeography remains to be determined. This could be informed by relations with vegetation structure and tree architecture. The fourth item can be derived from airborne or spaceborne LIDAR signal, as it has been demonstrated for selected sites (Taubert et al., 2021). However, scaling such study globally could prove challenging as relations might be context dependent.

Integrating the variability of these parameters (e.g., branches of different sizes) at the coarser simulation scale typical of Madingley could prove conceptually and computationally challenging. For instance, it could require switching from a monthly timestep to a daily or sub daily timestep, or switching from cohorts to individuals, to better account for animal interaction with the complexity of vegetation structure. Further studies could also inform about how species interact with plants architecture based on their specific traits (e.g.: body plan, mobility type, size, behavior), allowing for finer discrimination of animal strategies (Hao et al., 2021; Johnston & Smith, 2018; Killion et al., 2023b; Randlkofer et al., 2010; Russo et al., 2023).

Scale simplification

Because of the one-month time step, the grid cell resolution and the cohort approach of Madingley, we had to simplify the representation of vegetation structure and its interaction with animal population. This simplification is ecologically relevant, as we can, for instance, consider that over a one-month period, an individual will encounter branches of all sizes. Similarly, a cohort of N individuals (with a unique set of traits) can interact with N times more branches than a single individual. Thus, we can assume that the diversity of vegetation dimensions is fully sampled by each cohort, according to its mobility ability, at each time step, in each homogeneous grid cell. Computing the diversity of tree and branch sizes would either require intractable computation or produce odd patterns. Thus, we consider a unique architecture, based on the largest tree. This leads to animal use of vegetation structure to be both evened and maximized. Not doing so would reduce the supported animal biomass of simulated forested areas, bringing Madingley's output closer in range with TetraDENSITY's data. This could appear as a positive outcome; however, as we did not simulate human impact (but is inherently present in observations), we aim for higher simulated animal biomass than observed. There is a growing literature, and yet no consensus as to how much higher animal populations could be without human influence (de Thoisy et al., 2010; Hill et al., 2020; Pedersen et al., 2023; F. A. Smith et al., 2018, 2019; Toews et al., 2018). This effect is most likely context dependent and needs to be examined in the light of Madingley's inner geographic biases.

Our representation of animal populations interacting with vegetation structure focuses on the plant scale, but at the landscape scale other factors could be considered. For instance, habitat fragmentation and complexity likely shape assemblages of species. This represents an interaction between species specific traits (e.g. types of movement, metabolic rate, body size and body plan), and parameters of habitat fragmentation (gap size, gap complexity, type of habitat/activity impacted). Simulating all these factors is challenging and observations which could support such integration are still sparse. However, recent studies (Killion et al., 2023b; Russo et al., 2023) are informing us about such ecological processes and works such as Hansen et al., (2024) are paving the way forward. Integration in a mechanistic ecological model do not exist yet, to our knowledge, but should be achievable in the near future.

NPP organs partitioning

In Madingley, NPP is not distributed to different plant organs, thus, it overestimates what is available for herbivory as "leaves". This could be considered as representing other feeding strategies, such as ability to feed on sap, nectar, fruits, seeds, root exudates or dead plant matter. However, this is not partitioned in Madingley and is available to every cohort regardless of their body mass or any other trait. Further research would be required to design a comprehensive feeding module, considering each strategy individually. Mechanistic attempts at modelling feeding strategies, and their feedback on plant populations (Pachzelt et al., 2015; Pfeiffer et al., 2019), are existing, but none, to our knowledge, consider all the strategies simultaneously so far. This would represent a major step forward, but would require careful designing, to minimize the high computation cost it could require.

Largest tree, NPP pooling and feeding order

The largest tree approach, all other parameters being equal for each cohort, can be understood as each animal cohort having access to as much plant biomass as it can, and thus, as having optimized feeding order. This does not explicitly and directly modify competition and community assembly. Yet the more a cohort is successful, the more this approximation might favor it, given that it benefits all cohort proportionately. Simultaneously, this maximized NPP available is still impacted by actual computed feeding order, which is random, changing at each time step. Thus, depending on the number of cohorts simulated in a grid cell and the "life expectancy" of each given cohort, they are more or less statistically favored or disfavored. We have little information about feeding order to parameterize or benchmark this process. There is evidence about larger animal tending to feed first (Remis, 1995; Schoener, 2003), but we could not identify a comprehensive understanding of the magnitude of this effect. Without a mathematical explanation of this mechanism, considering its geographic patterns or explanation by traits or landscape features, we cannot integrate it in Madingley.

We approximate NPP distribution through the height column by allocating it to each height bin according to GEDI PAVD profile and along branches according to assumptions. For computation tractability, we did not split NPP into multiple pools, per height bin, and across branch length. The distribution of NPP is applied separately to each cohort when it feeds. Thus, while each cohort can access and feed on only a fraction of total NPP, it depletes the total NPP, which is ultimately available to every cohort. Predation functions on the same principle, but NPP is replaced by prey abundance density. Therefore, when feeding, order can be unrealistically important for the last feeding cohort, particularly if they are of the smaller arboreal type, as they get access to a much smaller fraction of available resources as they should, if considered in a vacuum. It might be possible to account for this effect by creating a pool of resources available per cohort (i.e.: a number of pool equal to the number of cohorts). This would require keeping track of each pool, as feeding order would impact them sequentially. While this solution is logically simple, it is computationally expensive and inefficient (e.g. causing memory issues). Another option, avoiding the computing issue could be to order feeding of cohorts based on their body size. Here we would have two options, both with a downfall. First, we could assume that larger animals feed first, as they have access to less resources in the canopy, due to their body size limitation, and thus they should not deplete the total pool. In the model, each large-bodied cohort would be unable to significantly deplete the total pool by itself, but, if there are too many large-bodied cohort, they could, altogether deplete the total pool. Additionally, this would reduce the advantage of smaller bodied cohorts, which while having access to the entire pool, would be left feeding on a smaller pool, as it would have been depleted by larger bodied cohorts feeding first. This would lead to the removal of the smallest cohorts in forest environment. Second, we could assume that smaller bodied cohorts would feed first, thus having access to has much resource as their

small bodies allow them too. This would be logical, and congruent with the assumption that being smaller in the canopy is favored over being larger, in order to maximize access to resources. However, this would imply that larger bodied cohorts would have access to an even smaller pool of resources, likely too small to support them. Both options, despite being computationally efficient, are not satisfactory as they rule out the end members of the body size spectrum.

Species behaviors

We assume that animals feed non-discriminatively across all the height bins they have access to. However, in real life, they are likely to access preferentially some layers, according to their movement capacity, behavioral habits and feeding preferences interaction with food distribution (De Guinea et al., 2019; Delciellos & Vieira, 2006; Dunbar & Badam, 2000; Hopkins, 2011; Mattingly & Jayne, 2004; McClearn, 1992; Milliken et al., 2005; Parker et al., 2022; Schaefer et al., 2002). Animal species traits interact with vertical plant traits differentiation; for example, leaves traits have been shown to vary vertically (Hagemeier & Leuschner, 2019), which could impact palatability and nutritional value. Evidence exists for feeding order favoring larger animals on the ground (Schoener, 2003), but this has not been implemented and evaluated in Madingley previously and we do not have observations on this mechanism for arboreal interactions. Additionally, animals able to access only the lowest non-ground layer might focus on ground available food and only marginally access branches (Emmons, 1987). Again, we are not able to integrate such behaviors at present, as data supporting it are still insufficient. Moreover, diverging strategies among cohorts and competition mechanisms (e.g.: an animal might access resource more efficiently than another by being faster, or avoiding competitors or scaring them away) are likely to interact with body mass feeding ordering as previously discussed, further obscuring our understanding of this mechanism.

Benchmarking Tetradensity

Assessing the validity and accuracy of our approach is challenging. Our implementation of vegetation structure in community assembly processes brings model results closer to observations, indicating that our approach is going in the right direction. However, a precise measure of this effect is challenging. We have note that the data we use as "observations" to benchmark our results, while being the best we could obtain, are having their own limitations. First, they are derived from site specific field studies and extrapolated at global scale to fill the gaps. Second, we did not consider species other than mammals and birds, as we have lower confidence in their abundance density estimates globally. Third, even for considered species, there are inherent limitations. For instance, the bird matrix is built considering only resident ranges and the breeding plus resident part of the range of migratory species. They do not include the non-breeding range. Thus, biomass map is seasonal. Considering both ranges would over-estimate biomass. Further refinement of these biomass abundance density estimates could solve that. However, this is of secondary concern here as biomass of birds is much smaller than biomass of mammals, and global endotherm biomass considered is mostly a reflection of the global biomass of mammals.

Predation

Integrating vegetation structure in Madingley modifies predation dynamics. Predators need to have their accessible branch space overlapping with their prey's accessible branch space. Predator space is typically smaller than prey space, as predators are coded to have higher body mass compared to their prey in Madingley. This implies a reduction of available prey for predators in 3D structured environment. As predators are typically larger than their prey, they do not have access to the entirety of the prey pool. The rationale for branch space availability in terms of predation is the same as for herbivory. Considering predation specificities, when considering predator body mass to calculate the branch space overlap between prey and predator, we do not add the prey body mass to the predator body mass to calculate breaking point. This follows the logic we use for herbivory, even though during a predation event, both individuals can be intuitively understood as standing at the same point along branch length. We assume that we can ignore this body mass addition during predation event as adaptation to predation across canopy space should limit the impact of this addition instead of increasing it. Further, we could assume that the added momentum implied by the predation behavior could further strain branches. We did not include this mechanism as any movement would add momentum to animal weight, but this is mediated by movement type and body plan, for which we have little data (van Casteren et al., 2013). We assume that these relations are negligible at the broad scale at which we performed our simulations.

CONCLUSION

Vegetation structure is increasingly recognized as a key variable explaining whole ecosystem state parameters, in particular biomass and NPP (R. Dubayah et al., 2022; Hawbaker et al., 2009; Muumbe et al., 2024; Ni-Meister et al., 2010), and dynamics (Bondeau et al., 1999; Hurtt et al., 2010; Plöchl & Cramer, 1995). We present here the first study to mechanistically model its cascading impact on animal community assembly. Our findings align with studies emphasizing the role of vegetation structure in habitat quality and trophic interactions, revealing its cascading effects on animal communities. We demonstrate that considering the most conservative assumptions and simplification to integrate vegetation structure in animal community assembly is sufficient to improve our ability to model this crucial ecological question. Recent works stress the urgency of improving forecasting amid accelerating climate and land use change as biogeographic patterns are re-shaped (Cui et al., 2021; Liao et al., 2021; Sousa-Guedes et al., 2020; Thompson et al., 2023; Trew & Maclean, 2021). Our study, emphasizing the need for vegetation structure integration, contributes to more accurate simulations of the cascading and interacting consequences of land cover change and community assembly. contributing to will be necessary. Thus, we provide an important contribution to our ability to inform our understanding of anthropogenic and climatic impacts on ecosystems globally, providing improved capabilities to inform decision making.

Acknowledgment

Support was provided by the GEDI mission and NASA Research Opportunities in Space and Earth Science Grants # 80NSSC20K0216, 80NSSC19K0206 and 80NSSC21K0191.

Authors contribution

C.G., M.H., A.A. and C.D. led the study. C.G. wrote the manuscript. C.G. and M.H. led the modelling component (coding, simulations, analyses). P.B. contributed the GEDI data analysis. L.C. contributed the TetraDensity analysis. P.J. contributed the Elton traits analysis. T.J. contributed the TLS data analysis. All authors contributed to the study and manuscript.

Conflict of interests

None

Data availability

Code is available at: https://github.com/Megabiota-Lab/MadingleyCPP-openMP-3D-V1.1

REFERENCES

Antony, F., Jordan, L., Schimleck, L. R., Clark, A., Souter, R. A., & Daniels, R. F. (2011). Regional variation in wood modulus of elasticity (stiffness) and modulus of rupture (strength) of planted loblolly pine in the United States. *Canadian Journal of Forest Research*, *41*(7), 1522–1533. https://doi.org/10.1139/X11-064/ASSET/IMAGES/LARGE/X11-064F8.JPEG

Atikah, S. N., Yahya, M. S., Norhisham, A. R., Kamarudin, N., Sanusi, R., & Azhar, B. (2021). Effects of vegetation structure on avian biodiversity in a selectively logged hill dipterocarp forest. *Global Ecology and Conservation*, *28*, e01660. https://doi.org/10.1016/J.GECCO.2021.E01660

Atkins, J. W., Walter, J. A., Stovall, A. E. L., Fahey, R. T., & Gough, C. M. (2022). Power law scaling relationships link canopy structural complexity and height across forest types. *Functional Ecology*, *36*(3), 713–726. https://doi.org/10.1111/1365-2435.13983

Baar, J., Tippner, J., & Rademacher, P. (2015). Prediction of mechanical properties - modulus of rupture and modulus of elasticity - of five tropical species by nondestructive methods. *Maderas. Ciencia y Tecnología*, *17*(2), 239–252. https://doi.org/10.4067/S0718-221X2015005000023

Barnosky, A. D., Matzke, N., Tomiya, S., Wogan, G. O. U., Swartz, B., Quental, T. B., Marshall, C., McGuire, J. L., Lindsey, E. L., Maguire, K. C., Mersey, B., & Ferrer, E. A. (2011). Has the Earth's sixth mass extinction already arrived? *Nature 2011 471:7336*, *471*(7336), 51–57. https://doi.org/10.1038/nature09678

Bergman, J., Pedersen, R., Lundgren, E. J., Lemoine, R. T., Monsarrat, S., Pearce, E. A., Schierup, M. H., & Svenning, J. C. (2023). Worldwide Late Pleistocene and Early Holocene population declines in extant megafauna are associated with Homo sapiens expansion rather than climate change. *Nature Communications 2023 14:1*, *14*(1), 1–11. https://doi.org/10.1038/s41467-023-43426-5

Bondeau, A., Haxeltine, A., Heimann, M., Hoffstadt, J., Kaduk, J., Kergoat, L., Kicklighter, D. W., Knorr, W., Kohlmaier, G., Lurin, B., Maisongrande, P., Martin, P., Mckeown, R., Meeson, B., Iii, B. M., Nemani, R., Nemry, B., Olson, R., Otto, R., … Fischer, A. (1999). Comparing global models of terrestrial net primary productivity (NPP): importance of vegetation structure on seasonal NPP estimates. *Global Change Biology*, *5*(S1), 35–45. https://doi.org/10.1046/J.1365-2486.1999.00005.X

Campos-Silva, L. A., & Piratelli, A. J. (2020). Vegetation structure drives taxonomic diversity and functional traits of birds in urban private native forest fragments. *Urban Ecosystems 2020 24:2*, *24*(2), 375–390. https://doi.org/10.1007/S11252-020-01045-8

Ceballos, G., Ehrlich, P. R., & Dirzo, R. (2017). Biological annihilation via the ongoing sixth mass extinction signaled by vertebrate population losses and declines. *Proceedings of the National Academy of Sciences of the United States of America*, *114*(30), E6089–E6096. https://doi.org/10.1073/pnas.1704949114

Collier, N., Hoffman, F. M., Lawrence, D. M., Keppel-Aleks, G., Koven, C. D., Riley, W. J., Mu, M., & Randerson, J. T. (2018). The International Land Model Benchmarking (ILAMB) System: Design, Theory, and Implementation. *Journal of Advances in Modeling Earth Systems*, *10*(11), 2731–2754. https://doi.org/10.1029/2018MS001354

Coverdale, T. C., & Davies, A. B. (2023). Unravelling the relationship between plant diversity and vegetation structural complexity: A review and theoretical framework. *Journal of Ecology*, *111*(7), 1378–1395. https://doi.org/10.1111/1365-2745.14068

Cowie, R. H., Bouchet, P., & Fontaine, B. (2022). The Sixth Mass Extinction: fact, fiction or speculation? *Biological Reviews*, *97*(2), 640–663. https://doi.org/10.1111/BRV.12816

Cui, D., Liang, S., & Wang, D. (2021). Observed and projected changes in global climate zones based on Köppen climate classification. *Wiley Interdisciplinary Reviews: Climate Change*, *12*(3), e701. https://doi.org/10.1002/WCC.701

Dahle, G. A., & Grabosky, J. C. (2010). Allometric patterns in Acer platanoides (Aceraceae) branches. *Trees - Structure and Function*, *24*(2), 321–326. https://doi.org/10.1007/S00468-009-0401-5/METRICS

De Guinea, M., Estrada, A., Nekaris, K. A. I., & Van Belle, S. (2019). Arboreal route navigation in a Neotropical mammal: Energetic implications associated with tree monitoring and landscape attributes. *Movement Ecology*, *7*(1), 1–12. https://doi.org/10.1186/S40462-019-0187-Z/FIGURES/3

de Thoisy, B., Richard-Hansen, C., Goguillon, B., Joubert, P., Obstancias, J., Winterton, P., & Brosse, S. (2010). Rapid evaluation of threats to biodiversity: Human footprint score and large vertebrate species responses in French Guiana. *Biodiversity and Conservation*, *19*(6), 1567–1584. https://doi.org/10.1007/S10531-010-9787-Z/FIGURES/6

Decuyper, M., Mulatu, K. A., Brede, B., Calders, K., Armston, J., Rozendaal, D. M. A., Mora, B., Clevers, J. G. P. W., Kooistra, L., Herold, M., & Bongers, F. (2018). Assessing the structural differences between tropical forest types using Terrestrial Laser Scanning. *Forest Ecology and Management*, *429*, 327–335. https://doi.org/10.1016/J.FORECO.2018.07.032

Delciellos, A. C., & Vieira, M. V. (2006). Arboreal walking performance in seven didelphid marsupials as an aspect of their fundamental niche. *Austral Ecology*, *31*(4), 449–457. https://doi.org/10.1111/J.1442-9993.2006.01604.X

Dohn, J., Augustine, D. J., Hanan, N. P., Ratnam, J., & Sankaran, M. (2017). Spatial vegetation patterns and neighborhood competition among woody plants in an East African savanna. *Ecology*. https://doi.org/10.1002/ecy.1659

Doughty, C. E., Gaillard, C., Burns, P., Keany, J. M., Abraham, A. J., Malhi, Y., Aguirre-Gutierrez, J., Koch, G., Jantz, P., Shenkin, A., & Tang, H. (2023). Tropical forests are mainly unstratified especially in Amazonia and regions with lower fertility or higher temperatures. *Environmental Research: Ecology*, *2*(3), 035002. https://doi.org/10.1088/2752-664X/ace723

Dubayah, R., Armston, J., Healey, S. P., Bruening, J. M., Patterson, P. L., Kellner, J. R., Duncanson, L., Saarela, S., Ståhl, G., Yang, Z., Tang, H., Blair, J. B., Fatoyinbo, L., Goetz, S., Hancock, S., Hansen, M., Hofton, M., Hurtt, G., & Luthcke, S. (2022). GEDI launches a new era of biomass inference from space. *Environmental Research Letters*, *17*(9), 095001. https://doi.org/10.1088/1748-9326/AC8694

Dubayah, R., Blair, J. B., Goetz, S., Fatoyinbo, L., Hansen, M., Healey, S., Hofton, M., Hurtt, G., Kellner, J., Luthcke, S., Armston, J., Tang, H., Duncanson, L., Hancock, S., Jantz, P., Marselis, S., Patterson, P. L., Qi, W., & Silva, C. (2020). The Global Ecosystem Dynamics Investigation: High-resolution laser ranging of the Earth's forests and topography. *Science of Remote Sensing*, *1*, 100002. https://doi.org/10.1016/j.srs.2020.100002

Dubayah, R., Hofton, M., Blair, J., Armston, J., Tang, H., & Luthcke, S. (2021). GEDI L2A Elevation and Height Metrics Data Global Footprint Level V002. In *Data set*. NASA EOSDIS Land Processes Distributed Active Archive Center. https://doi.org/https://doi.org/10.5067/GEDI/GEDI02_A.002

Dubayah, R. O., Armston, J., Healey, S. P., Yang, Z., Patterson, P. L., Saarela, S., Stahl, G., Duncanson, L., & Kellner, J. R. (2022). GEDI L4B Gridded Aboveground Biomass Density, Version 2. In *Dataset*. ORNL DAAC.

Dubayah, R., Tang, H., Armston J., Luthcke S., Hofton M., & Blair J. (2021). GEDI L2B Canopy Cover and Vertical Profile Metrics Data Global Footprint Level V002. In *Data set*. NASA EOSDIS Land Processes Distributed Active Archive Center. https://doi.org/https://doi.org/10.5067/GEDI/GEDI02_B.002

Dunbar, D. C., & Badam, G. L. (2000). Locomotion and posture during terminal branch feeding. *International Journal of Primatology*, *21*(4), 649–669. https://doi.org/10.1023/A:1005565304671/METRICS

Emmons, L. H. (1987). Comparative feeding ecology of felids in a neotropical rainforest. *Behavioral Ecology and Sociobiology*, *20*(4), 271–283. https://doi.org/10.1007/BF00292180/METRICS

Enquist, B. J., & Niklas, K. J. (2001). Invariant scaling relations across tree-dominated communities. *Nature*, *410*(6829), 655–660.

Eyring, V., Bony, S., Meehl, G. A., Senior, C. A., Stevens, B., Stouffer, R. J., & Taylor, K. E. (2016). Overview of the Coupled Model Intercomparison Project Phase 6 (CMIP6) experimental design and organization. *Geoscientific Model Development*, *9*(5), 1937–1958. https://doi.org/10.5194/gmd-9-1937-2016

Felton, A., Felton, A. M., Wood, J., & Lindenmayer, D. B. (2006). Vegetation structure, phenology, and regeneration in the natural and anthropogenic tree-fall gaps of a reduced-impact logged subtropical Bolivian forest. *Forest Ecology and Management*, *235*(1–3), 186–193. https://doi.org/10.1016/J.FORECO.2006.08.011

Franklin, O., Harrison, S. P., Dewar, R., Farrior, C. E., Brännström, Å., Dieckmann, U., Pietsch, S., Falster, D., Cramer, W., Loreau, M., Wang, H., Mäkelä, A., Rebel, K. T., Meron, E., Schymanski, S. J., Rovenskaya, E., Stocker, B. D., Zaehle, S., Manzoni, S., … Prentice, I. C. (2020). Organizing principles for vegetation dynamics. *Nature Plants 2020 6:5*, *6*(5), 444–453. https://doi.org/10.1038/s41477-020-0655-x

Gámez, S., & Harris, N. C. (2022). Conceptualizing the 3D niche and vertical space use. *Trends in Ecology & Evolution*, *37*(11), 953–962. https://doi.org/10.1016/J.TREE.2022.06.012

Haberl, H., Erb, K. H., Krausmann, F., Gaube, V., Bondeau, A., Plutzar, C., Gingrich, S., Lucht, W., & Fischer-Kowalski, M. (2007). Quantifying and mapping the human appropriation of net primary production in earth's terrestrial ecosystems. *Proceedings of the National Academy of Sciences of the United States of America*, *104*(31), 12942–12947. https://doi.org/10.1073/PNAS.0704243104/SUPPL_FILE/INDEX.HTML

Hackenberg, J., Spiecker, H., Calders, K., Disney, M., & Raumonen, P. (2015). SimpleTree —An Efficient Open Source Tool to Build Tree Models from TLS Clouds. *Forests 2015, Vol. 6, Pages 4245-4294*, *6*(11), 4245–4294. https://doi.org/10.3390/F6114245

Hagemeier, M., & Leuschner, C. (2019). Functional Crown Architecture of Five Temperate Broadleaf Tree Species: Vertical Gradients in Leaf Morphology, Leaf Angle, and Leaf Area Density. *Forests 2019, Vol. 10, Page 265*, *10*(3), 265. https://doi.org/10.3390/F10030265

Hansen, A. J., Aragon-Osejo, J., González, I., Veneros, J., Virnig, A. L. S., Jantz, P., Venter, O., Goetz, S., Watson, J. E. M., Cordoba, N., Rodriguez, S., Monroy, L., Iglesias, J., Beltrán, L., Borja, D., Ureta, D., Tingo, J., Oñate, C., Valencia, F., … Huerta, P. (2024). Developing national complementary indicators of SDG15 that consider forest quality: Applications in Colombia, Ecuador, and Peru. *Ecological Indicators*, *159*, 111654. https://doi.org/10.1016/J.ECOLIND.2024.111654

Hao, Z., Wang, C., Sun, Z., Zhao, D., Sun, B., Wang, H., & Konijnendijk Van Den Bosch, C. (2021). Vegetation structure and temporality influence the dominance, diversity, and composition of forest acoustic communities. *Forest Ecology and Management*, *482*, 118871. https://doi.org/10.1016/j.foreco.2020.118871

Harfoot, M. B. J., Newbold, T., Tittensor, D. P., Emmott, S., Hutton, J., Lyutsarev, V., Smith, M. J., Scharlemann, J. P. W., & Purves, D. W. (2014). Emergent Global Patterns of Ecosystem Structure and Function from a Mechanistic General Ecosystem Model. *PLOS Biology*, *12*(4), e1001841. https://doi.org/10.1371/JOURNAL.PBIO.1001841

Hawbaker, T. J., Keuler, N. S., Lesak, A. A., Gobakken, T., Contrucci, K., & Radeloff, V. C. (2009). Improved estimates of forest vegetation structure and biomass with a LiDAR-optimized sampling design. *Journal of Geophysical Research: Biogeosciences*, *114*(G2), 0–04. https://doi.org/10.1029/2008JG000870

Heit, D. R., Ortiz-Calo, W., & Montgomery, R. A. (2021). Landscape complexity persists as a critical source of bias in terrestrial animal home range estimation. *Ecology*, e03427. https://doi.org/10.1002/ECY.3427

Hill, J. E., DeVault, T. L., Wang, G., & Belant, J. L. (2020). Anthropogenic mortality in mammals increases with the human footprint. *Frontiers in Ecology and the Environment*, *18*(1), 13–18. https://doi.org/10.1002/FEE.2127

Høibø, O., & Vestøl, G. I. (2010). Modelling the variation in modulus of elasticity and modulus of rupture of scots pine round timber. *Canadian Journal of Forest Research*, *40*(4), 668–678. https://doi.org/10.1139/X10-021/ASSET/IMAGES/X10-021IE13H.GIF

Hopkins, M. E. (2011). Mantled Howler (Alouatta palliata) Arboreal Pathway Networks: Relative Impacts of Resource Availability and Forest Structure. *International Journal of Primatology*, *32*(1), 238–258. https://doi.org/10.1007/S10764-010-9464-9/TABLES/5

Hurtt, G. C., Fisk, J., Thomas, R. Q., Dubayah, R., Moorcroft, P. R., & Shugart, H. H. (2010). Linking models and data on vegetation structure. *Journal of Geophysical Research: Biogeosciences*, *115*(G2), 0–10. https://doi.org/10.1029/2009JG000937

Ishii, H. T., Tanabe, S., & Hiura, T. (2004). Exploring the Relationships Among Canopy Structure, Stand Productivity, and Biodiversity of Temperate Forest Ecosystems. *Forest Science*, *50*(3), 342–355. https://doi.org/10.1093/FORESTSCIENCE/50.3.342

IUCN. (2022). *The IUCN Red List of Ecosystems. Version 2022-1*. Https://Www.Iucnredlist.Org.

Jackson, T., Shenkin, A., Moore, J., Bunce, A., Van Emmerik, T., Kane, B., Burcham, D., James, K., Selker, J., Calders, K., Origo, N., Disney, M., Burt, A., Wilkes, P., Raumonen, P., Gonzalez De Tanago Menaca, J., Lau, A., Herold, M., Goodman, R. C., … Malhi, Y. (2019). An architectural understanding of natural sway frequencies in trees. *Journal of the Royal Society Interface*, *16*(155). https://doi.org/10.1098/rsif.2019.0116

Jantz, P., Abraham, A., Scheffers, B., Gaillard, C., Harfoot, M., Goetz, S., & Doughty, C. (n.d.). Functional traits and phylogeny predict vertical foraging in terrestrial mammals and birds. *In Prep*.

Jantz, P., Abraham, A., Scheffers, B., Gaillard, C., Harfoot, M., Goetz, S., & Doughty, C. E. (2024). Functional traits and phylogeny predict vertical foraging in terrestrial mammals and birds. *BioRxiv*, 2024.04.18.589860. https://doi.org/10.1101/2024.04.18.589860

Johnston, C. A., & Smith, R. S. (2018). Vegetation structure mediates a shift in predator avoidance behavior in a range-edge population. *Behavioral Ecology*, *29*(5), 1124–1131. https://doi.org/10.1093/BEHECO/ARY075

Just, M. G., Hohmann, M. G., & Hoffmann, W. A. (2016). Where fire stops: vegetation structure and microclimate influence fire spread along an ecotonal gradient. *Plant Ecology*, *217*(6), 631–644. https://doi.org/10.1007/S11258-015-0545-X/FIGURES/5

Keany, J. M., Burns, P., Abraham, A. J., Jantz, P., Makaga, L., Saatchi, S., Maisels, F., Abernethy, K., & Doughty, C. (2023). Using a multiscale lidar approach to determine variation in canopy structure from African forest elephant trails. *BioRxiv*, 2023.08.25.554381. https://doi.org/10.1101/2023.08.25.554381

Killion, A. K., Honda, A., Trout, E., & Carter, N. H. (2023a). Integrating spaceborne estimates of structural diversity of habitat into wildlife occupancy models. *Environmental Research Letters*, *18*(6), 065002. https://doi.org/10.1088/1748-9326/ACCE4D

Killion, A. K., Honda, A., Trout, E., & Carter, N. H. (2023b). Integrating spaceborne estimates of structural diversity of habitat into wildlife occupancy models. *Environmental Research Letters*, *18*(6), 065002. https://doi.org/10.1088/1748-9326/ACCE4D

Krausmann, F., Erb, K. H., Gingrich, S., Haberl, H., Bondeau, A., Gaube, V., Lauk, C., Plutzar, C., & Searchinger, T. D. (2013). Global human appropriation of net primary production doubled in the 20th century. *Proceedings of the National Academy of Sciences of the United States of America*, *110*(25), 10324–10329. https://doi.org/10.1073/PNAS.1211349110/SUPPL_FILE/SAPP.PDF

Lau, A., Martius, C., Bartholomeus, H., Shenkin, A., Jackson, T., Malhi, Y., Herold, M., & Bentley, L. P. (2019a). Estimating architecture-based metabolic scaling exponents of tropical trees using terrestrial LiDAR and 3D modelling. *Forest Ecology and Management*, *439*, 132–145. https://doi.org/10.1016/J.FORECO.2019.02.019

Lau, A., Martius, C., Bartholomeus, H., Shenkin, A., Jackson, T., Malhi, Y., Herold, M., & Bentley, L. P. (2019b). Estimating architecture-based metabolic scaling exponents of tropical trees using terrestrial LiDAR and 3D modelling. *Forest Ecology and Management*, *439*(September 2018), 132–145. https://doi.org/10.1016/j.foreco.2019.02.019

Lemoine, R. T., Buitenwerf, R., & Svenning, J.-C. (2023). Megafauna extinctions in the late-Quaternary are linked to human range expansion, not climate change. *Anthropocene*, *44*, 100403. https://doi.org/10.1016/j.ancene.2023.100403

Leu, M., Hanser, S. E., & Knick, S. T. (2008). The human footprint in the West: A large-scale analysis of anthropogenic impacts. *Ecological Applications*, *18*(5), 1119–1139. https://doi.org/10.1890/07-0480.1

Liao, M. ling, Li, G. yang, Wang, J., Marshall, D. J., Hui, T. Y., Ma, S. yang, Zhang, Y. min, Helmuth, B., & Dong, Y. wei. (2021). Physiological determinants of biogeography: The importance of metabolic depression to heat tolerance. *Global Change Biology*, *27*(11), 2561–2579. https://doi.org/10.1111/GCB.15578

Lieth, H. (1973). Primary production: Terrestrial ecosystems. *Human Ecology*, *1*(4), 303–332. https://doi.org/10.1007/BF01536729/METRICS

Lu, Y., Wang, H., Zhang, Y., Liu, J., Qu, T., Zhao, X., Tian, H., Su, J., Luo, D., & Yang, Y. (2023). Combining Spatial–Temporal Remote Sensing and Human Footprint Indices to Identify Biodiversity Conservation Hotspots. *Diversity 2023, Vol. 15, Page 1064*, *15*(10), 1064. https://doi.org/10.3390/D15101064

MacArthur, R. H., & MacArthur, J. W. (1961). On Bird Species Diversity. *Ecology*, *42*(3), 594–598. https://doi.org/10.2307/1932254

Mace, G. M., Reyers, B., Alkemade, R., Biggs, R., Chapin, F. S., Cornell, S. E., Díaz, S., Jennings, S., Leadley, P., Mumby, P. J., Purvis, A., Scholes, R. J., Seddon, A. W. R., Solan, M., Steffen, W., & Woodward, G. (2014). Approaches to defining a planetary boundary for biodiversity. *Global Environmental Change*, *28*(1), 289–297. https://doi.org/10.1016/J.GLOENVCHA.2014.07.009

Martínez Cano, I., Shevliakova, E., Malyshev, S., Wright, S. J., Detto, M., Pacala, S. W., & Muller-Landau, H. C. (2020). Allometric constraints and competition enable the simulation of size structure and carbon fluxes in a dynamic vegetation model of tropical forests (LM3PPA-TV). *Global Change Biology*, *26*(8), 4478–4494. https://doi.org/10.1111/GCB.15188

Mattingly, W. B., & Jayne, B. C. (2004). Resource use in arboreal habitats: structure affects locomotion of four ecomorphs of anolis lizards. *Ecology*, *85*(4), 1111–1124. https://doi.org/10.1890/03-0293

McClearn, D. (1992). Locomotion, Posture, and Feeding Behavior of Kinkajous, Coatis, and Raccoons. *Journal of Mammalogy*, *73*(2), 245–261. https://doi.org/10.2307/1382055

McElhinny, C., Gibbons, P., Brack, C., & Bauhus, J. (2005). Forest and woodland stand structural complexity: Its definition and measurement. *Forest Ecology and Management*, *218*(1–3), 1–24. https://doi.org/10.1016/J.FORECO.2005.08.034

Migliavacca, M., Musavi, T., Mahecha, M. D., Nelson, J. A., Knauer, J., Baldocchi, D. D., Perez-Priego, O., Christiansen, R., Peters, J., Anderson, K., Bahn, M., Black, T. A., Blanken, P. D., Bonal, D., Buchmann, N., Caldararu, S., Carrara, A., Carvalhais, N., Cescatti, A., … Reichstein, M. (2021a). The three major axes of terrestrial ecosystem function. *Nature*, *598*(7881), 468–472. https://doi.org/10.1038/s41586-021-03939-9

Migliavacca, M., Musavi, T., Mahecha, M. D., Nelson, J. A., Knauer, J., Baldocchi, D. D., Perez-Priego, O., Christiansen, R., Peters, J., Anderson, K., Bahn, M., Black, T. A., Blanken, P. D., Bonal, D., Buchmann, N., Caldararu, S., Carrara, A., Carvalhais, N., Cescatti, A., … Reichstein, M. (2021b). The three major axes of terrestrial ecosystem function. *Nature 2021 598:7881*, *598*(7881), 468–472. https://doi.org/10.1038/s41586-021-03939-9

Milliken, G. W., Ferra, G., Kraiter, K. S., & Ross, C. L. (2005). Reach and posture hand preferences during arboreal feeding in sifakas (Propithecus sp.): A test of the postural origins theory of behavioral lateralization. *Journal of Comparative Psychology*, *119*(4), 430–439. https://doi.org/10.1037/0735-7036.119.4.430

Moore, J., Achim, A., Lyon, A., Mochan, S., & Gardiner, B. (2009). Effects of early re-spacing on the physical and mechanical properties of Sitka spruce structural timber. *Forest Ecology and Management*, *258*(7), 1174–1180. https://doi.org/10.1016/j.foreco.2009.06.009

Moorthy, S. M. K., Calders, K., e Brugnera, M. di P., Schnitzer, S. A., & Verbeeck, H. (2018). Terrestrial Laser Scanning to Detect Liana Impact on Forest Structure. *Remote Sensing 2018, Vol. 10, Page 810*, *10*(6), 810. https://doi.org/10.3390/RS10060810

Muumbe, T. P., Singh, J., Baade, J., Raumonen, P., Coetsee, C., Thau, C., & Schmullius, C. (2024). Individual Tree-Scale Aboveground Biomass Estimation of Woody Vegetation in a Semi-Arid Savanna Using 3D Data. *Remote Sensing*, *16*(2), 399. https://doi.org/10.3390/RS16020399/S1

Nelson, A. S., Weiskittel, A. R., & Wagner, R. G. (2014). Development of branch, crown, and vertical distribution leaf area models for contrasting hardwood species in Maine, USA. *Trees - Structure and Function*, *28*(1), 17–30. https://doi.org/10.1007/s00468-013-0926-5

Newbold, T., Hudson, L. N., Arnell, A. P., Contu, S., De Palma, A., Ferrier, S., Hill, S. L. L., Hoskins, A. J., Lysenko, I., Phillips, H. R. P., Burton, V. J., Chng, C. W. T., Emerson, S., Gao, D., Hale, G. P., Hutton, J., Jung, M., Sanchez-Ortiz, K., Simmons, B. I., … Purvis, A. (2016). Has land use pushed terrestrial biodiversity beyond the planetary boundary? A global assessment. *Science*, *353*(6296), 291–288. https://doi.org/10.1126/SCIENCE.AAF2201/SUPPL_FILE/NEWBOLD-SM.PDF

Newbold, T., Tittensor, D. P., Harfoot, M. B. J., Scharlemann, J. P. W., & Purves, D. W. (2020). Non-linear changes in modelled terrestrial ecosystems subjected to perturbations. *Scientific Reports*, *10*(1), 14051. https://doi.org/10.1038/s41598-020-70960-9

Niklas, K. J., & Spatz, H.-C. (2012). *Plant physics* [Book]. University of Chicago Press. https://doi.org/10.7208/9780226586342

Ni-Meister, W., Lee, S., Strahler, A. H., Woodcock, C. E., Schaaf, C., Yao, T., Ranson, K. J., Sun, G., & Blair, J. B. (2010). Assessing general relationships between aboveground biomass and vegetation structure parameters for improved carbon estimate from lidar remote sensing. *Journal of Geophysical Research: Biogeosciences*, *115*(G2), 0–11. https://doi.org/10.1029/2009JG000936

Pachzelt, A., Forrest, M., Rammig, A., Higgins, S. I., & Hickler, T. (2015). Potential impact of large ungulate grazers on African vegetation, carbon storage and fire regimes. *Global Ecology and Biogeography*, *24*(9), 991–1002. https://doi.org/10.1111/geb.12313

Parker, E. J., Hill, R. A., & Koyama, N. F. (2022). Behavioral responses to spatial variation in perceived predation risk and resource availability in an arboreal primate. *Ecosphere*, *13*(2), e3945. https://doi.org/10.1002/ECS2.3945

Pedersen, R. Ø., Faurby, S., & Svenning, J. C. (2023). Late-Quaternary megafauna extinctions have strongly reduced mammalian vegetation consumption. *Global Ecology and Biogeography*, *32*(10), 1814–1826. https://doi.org/10.1111/GEB.13723

Pfeiffer, M., Langan, L., Linstädter, A., Martens, C., Gaillard, C., Ruppert, J. C., Higgins, S. I., Mudongo, E. I., & Scheiter, S. (2019). Grazing and aridity reduce perennial grass abundance in semi-arid rangelands – Insights from a trait-based dynamic vegetation model. *Ecological Modelling*, *395*, 11–22. https://doi.org/10.1016/J.ECOLMODEL.2018.12.013

Plöchl, M., & Cramer, W. (1995). Coupling global models of vegetation structure and ecosystem processes. *Tellus B*, *47*(1–2), 240–250. https://doi.org/10.1034/J.1600-0889.47.ISSUE1.20.X

Prentice, I. C., Bondeau, A., Cramer, W., Harrison, S. P., Hickler, T., Lucht, W., Sitch, S., Smith, B., & Sykes, M. T. (2007). Dynamic Global Vegetation Modeling: Quantifying Terrestrial Ecosystem

Responses to Large-Scale Environmental Change. In *Terrestrial Ecosystems in a Changing World* (pp. 175–192). Springer Berlin Heidelberg. https://doi.org/10.1007/978-3-540-32730-1_15

Prentice, I. C., Liang, X., Medlyn, B. E., & Wang, Y.-P. (2015). Reliable, robust and realistic: the three R's of next-generation land-surface modelling. *Atmospheric Chemistry and Physics*, *15*(10), 5987–6005. https://doi.org/10.5194/acp-15-5987-2015

Purves, D., Scharlemann, J. P. W., Harfoot, M., Newbold, T., Tittensor, D. P., Hutton, J., & Emmott, S. (2013). Ecosystems: Time to model all life on Earth. In *Nature* (Vol. 493, Issue 7432, pp. 295–297). Nature Publishing Group. https://doi.org/10.1038/493295a

Rahardjo Daryl Lee Tsen-Tieng, H. (2014). *Study of the modulus of rupture and modulus of elasticity of green wood of local tree species*. 2013–2027. https://dr.ntu.edu.sg/handle/10356/105512

Randlkofer, B., Obermaier, E., Hilker, M., & Meiners, T. (2010). Vegetation complexity-The influence of plant species diversity and plant structures on plant chemical complexity and arthropods. In *Basic and Applied Ecology* (Vol. 11, Issue 5, pp. 383–395). https://doi.org/10.1016/j.baae.2010.03.003

Raumonen, P., Kaasalainen, M., Markku, Å., Kaasalainen, S., Kaartinen, H., Vastaranta, M., Holopainen, M., Disney, M., & Lewis, P. (2013). Fast Automatic Precision Tree Models from Terrestrial Laser Scanner Data. *Remote Sensing 2013, Vol. 5, Pages 491-520*, *5*(2), 491–520. https://doi.org/10.3390/RS5020491

Remis, M. (1995). Effects of body size and social context on the arboreal activities of lowland gorillas in the Central African Republic. *American Journal of Physical Anthropology*, *97*(4), 413–433. https://doi.org/10.1002/ajpa.1330970408

Rockström, J., Steffen, W., Noone, K., Persson, Å., Chapin, F. S., Lambin, E., Lenton, T. M., Scheffer, M., Folke, C., Schellnhuber, H. J., Nykvist, B., De Wit, C. A., Hughes, T., Van Der Leeuw, S., Rodhe, H., Sörlin, S., Snyder, P. K., Costanza, R., Svedin, U., … Walker, B. (2009). *Planetary Boundaries: Exploring the Safe Operating Space for Humanity* (Vol. 14, Issue 2). https://about.jstor.org/terms

Russo, N. J., Davies, A. B., Blakey, R. V., Ordway, E. M., & Smith, T. B. (2023). Feedback loops between 3D vegetation structure and ecological functions of animals. *Ecology Letters*, *26*(9), 1597–1613. https://doi.org/10.1111/ele.14272

Salas-López, A., Violle, C., Munoz, F., Menzel, F., & Orivel, J. (2022). Effects of Habitat and Competition on Niche Partitioning and Community Structure in Neotropical Ants. *Frontiers in Ecology and Evolution*, *10*, 863080. https://doi.org/10.3389/FEVO.2022.863080/BIBTEX

Sandom, C., Faurby, S., Sandel, B., & Svenning, J. C. (2014). Global late Quaternary megafauna extinctions linked to humans, not climate change. *Proceedings of the Royal Society B: Biological Sciences*, *281*(1787). https://doi.org/10.1098/rspb.2013.3254

Santini, L., Benítez-López, A., Dormann, C. F., & Huijbregts, M. A. J. (2022). Population density estimates for terrestrial mammal species. *Global Ecology and Biogeography*, *31*(5), 978–994. https://doi.org/10.1111/GEB.13476

Santini, L., Isaac, N. J. B., & Ficetola, G. F. (2018). TetraDENSITY: A database of population density estimates in terrestrial vertebrates. *Global Ecology and Biogeography*, *27*(7), 787–791. https://doi.org/10.1111/geb.12756

Santini, L., Tobias, J. A., Callaghan, C., Gallego-Zamorano, J., & Benítez-López, A. (2023). Global patterns and predictors of avian population density. *Global Ecology and Biogeography*, *32*(7), 1189–1204. https://doi.org/10.1111/GEB.13688

Schaefer, H. M., Schmidt, V., & Wesenberg, J. (2002). Vertical Stratification and Caloric Content of the Standing Fruit Crop in a Tropical Lowland Forest. *Biotropica*, *34*(2), 244–253. https://doi.org/10.1111/j.1744-7429.2002.tb00535.x

Schoener, T. W. (2003). Theory of Feeding Strategies. *Https://Doi.Org/10.1146/Annurev.Es.02.110171.002101*, *2*(1), 369–404. https://doi.org/10.1146/ANNUREV.ES.02.110171.002101

Smith, F. A., Elliott Smith, R. E., Lyons, S. K., Payne, J. L., & Villaseñor, A. (2019). The accelerating influence of humans on mammalian macroecological patterns over the late Quaternary. *Quaternary Science Reviews*, *211*, 1–16. https://doi.org/10.1016/J.QUASCIREV.2019.02.031

Smith, F. A., Smith, R. E. E., Lyons, S. K., & Payne, J. L. (2018). Body size downgrading of mammals over the late Quaternary. *Science*, *360*(6386), 310–313. https://doi.org/10.1126/SCIENCE.AAO5987/SUPPL_FILE/AAO5987-SMITH-SM.PDF

Smith, M. J., Purves, D. W., Vanderwel, M. C., Lyutsarev, V., & Emmott, S. (2013). The climate dependence of the terrestrial carbon cycle, including parameter and structural uncertainties. *Biogeosciences*, *10*(1), 583–606. https://doi.org/10.5194/bg-10-583-2013

Smith, W. K., & Berry, Z. C. (2013). Sunflecks? *Tree Physiology*, *33*(3), 233–237. https://doi.org/10.1093/TREEPHYS/TPT005

Sousa-Guedes, D., Arenas-Castro, S., & Sillero, N. (2020). Ecological Niche Models Reveal Climate Change Effect on Biogeographical Regions: The Iberian Peninsula as a Case Study. *Climate 2020, Vol. 8, Page 42*, *8*(3), 42. https://doi.org/10.3390/CLI8030042

Srivastava, D. S. (2006). Habitat structure, trophic structure and ecosystem function: Interactive effects in a bromeliad-insect community. *Oecologia*, *149*(3), 493–504. https://doi.org/10.1007/S00442-006-0467-3/FIGURES/6

Stark, S. C., Enquist, B. J., Saleska, S. R., Leitold, V., Schietti, J., Longo, M., Alves, L. F., Camargo, P. B., & Oliveira, R. C. (2015). Linking canopy leaf area and light environments with tree size distributions to explain Amazon forest demography. *Ecology Letters*, *18*(7), 636–645. https://doi.org/10.1111/ELE.12440

Stewart, M., Carleton, W. C., & Groucutt, H. S. (2021). Climate change, not human population growth, correlates with Late Quaternary megafauna declines in North America. *Nature Communications*, *12*(1), 965. https://doi.org/10.1038/s41467-021-21201-8

Taubert, F., Fischer, R., Knapp, N., & Huth, A. (2021). Deriving Tree Size Distributions of Tropical Forests from Lidar. *Remote Sensing*, *13*(1), 131. https://doi.org/10.3390/rs13010131

Thompson, L. M., Thurman, L. L., Cook, C. N., Beever, E. A., Sgrò, C. M., Battles, A., Botero, C. A., Gross, J. E., Hall, K. R., Hendry, A. P., Hoffmann, A. A., Hoving, C., LeDee, O. E., Mengelt, C., Nicotra, A. B., Niver, R. A., Pérez-Jvostov, F., Quiñones, R. M., Schuurman, G. W., … Whiteley, A. (2023). Connecting research and practice to enhance the evolutionary potential of species under climate change. *Conservation Science and Practice*, *5*(2), e12855. https://doi.org/10.1111/CSP2.12855

Tilman, D., Isbell, F., & Cowles, J. M. (2014). Biodiversity and Ecosystem Functioning. *Https://Doi.Org/10.1146/Annurev-Ecolsys-120213-091917*, *45*, 471–493. https://doi.org/10.1146/ANNUREV-ECOLSYS-120213-091917

Toews, M., Juanes, F., & Burton, A. C. (2018). Mammal responses to the human footprint vary across species and stressors. *Journal of Environmental Management*, *217*, 690–699. https://doi.org/10.1016/J.JENVMAN.2018.04.009

Trew, B. T., & Maclean, I. M. D. (2021). Vulnerability of global biodiversity hotspots to climate change. *Global Ecology and Biogeography*, *30*(4), 768–783. https://doi.org/10.1111/GEB.13272

van Casteren, A., Sellers, W. I., Thorpe, S. K. S., Coward, S., Crompton, R. H., & Ennos, A. R. (2013). Factors Affecting the Compliance and Sway Properties of Tree Branches Used by the Sumatran Orangutan (Pongo abelii). *PLOS ONE*, *8*(7), e67877. https://doi.org/10.1371/JOURNAL.PONE.0067877

Veenendaal, E. M., Torello-Raventos, M., Miranda, H. S., Sato, N. M., Oliveras, I., van Langevelde, F., Asner, G. P., & Lloyd, J. (2018). On the relationship between fire regime and vegetation structure in the tropics. *New Phytologist*, *218*(1), 153–166. https://doi.org/10.1111/nph.14940

Verbeeck, H., Bauters, M., Jackson, T., Shenkin, A., Disney, M., & Calders, K. (2019). Time for a Plant Structural Economics Spectrum. *Frontiers in Forests and Global Change*, *2*, 43. https://doi.org/10.3389/ffgc.2019.00043

Vose, J. M., Clinton, B. D., Sullivan, N. H., & Bolstad, P. V. (1995). Vertical leaf area distribution, light transmittance, and application of the Beer–Lambert Law in four mature hardwood stands in the southern Appalachians. *Canadian Journal of Forest Research*, *25*(6), 1036–1043. https://doi.org/10.1139/x95-113

Watson, J. E. M., & Venter, O. (2019). Mapping the Continuum of Humanity's Footprint on Land. In *One Earth* (Vol. 1, Issue 2, pp. 175–180). Cell Press. https://doi.org/10.1016/j.oneear.2019.09.004

Way, D. A., & Pearcy, R. W. (2012). Sunflecks in trees and forests: from photosynthetic physiology to global change biology. *Tree Physiology*, *32*(9), 1066–1081. https://doi.org/10.1093/TREEPHYS/TPS064

West, G. B., Enquist, B. J., & Brown, J. H. (2009). A general quantitative theory of forest structure and dynamics. *Proceedings of the National Academy of Sciences of the United States of America*, *106*(17), 7040–7045. https://doi.org/10.1073/pnas.0812294106

Wilman, H., Belmaker, J., Simpson, J., de la Rosa, C., Rivadeneira, M. M., & Jetz, W. (2014). EltonTraits 1.0: Species-level foraging attributes of the world's birds and mammals. *Ecology*, *95*(7), 2027–2027. https://doi.org/10.1890/13-1917.1

Woolmer, G., Trombulak, S. C., Ray, J. C., Doran, P. J., Anderson, M. G., Baldwin, R. F., Morgan, A., & Sanderson, E. W. (2008). Rescaling the Human Footprint: A tool for conservation planning at an ecoregional scale. *Landscape and Urban Planning*, *87*(1), 42–53. https://doi.org/10.1016/J.LANDURBPLAN.2008.04.005

Wu, D., Liu, Q. X., Xia, R. L., & Li, T. (2022). Study on the changes in vegetation structural coverage and its response mechanism to hydrology. *Open Geosciences*, *14*(1), 79–88. https://doi.org/10.1515/GEO-2020-0322/MACHINEREADABLECITATION/RIS

Ye, Y., Hu, C., Jiang, Y., Davison, G. W. H., & Ding, C. (2021). Three-dimensional niche partitioning between two colonially nesting ardeid species in central China. *Avian Research*, *12*(1), 1–8. https://doi.org/10.1186/S40657-021-00264-7/TABLES/1

Zhu, Q., Jiang, H., Peng, C., Liu, J., Fang, X., Wei, X., Liu, S., & Zhou, G. (2012). Effects of future climate change, CO2 enrichment, and vegetation structure variation on hydrological processes in China. *Global and Planetary Change*, *80–81*, 123–135. https://doi.org/10.1016/J.GLOPLACHA.2011.10.010